

1

Fundamentals of Magnetism

Jun Yamauchi

1.1 Magnetism of Materials

1.1.1 Historical Background

Magnets play a crucial role in a modern life; as we know, a vast number of devices are employed in the electromagnetic industry. In ancient times human beings experienced magnetic phenomena by utilizing natural iron minerals, especially magnetite. It was not until modern times that magnetic phenomena were appreciated from the standpoint of electromagnetics, to which many physicists such as Oersted and Faraday made a great contribution. In particular, Ampère explained magnetic materials in 1822, based on a small circular electric current. This was the first explanation of a molecular magnet. Furthermore, Ampère's circuital law introduced the concept of a magnetic moment or magnetic dipoles, similar to electric dipoles. Macroscopic electromagnetic phenomena are depicted in Figure 1.1, in which a bar magnet and a circuital current in a wire are physically equivalent. Microscopic similarity is shown in Figure 1.2, in which a magnetic moment or dipole and a microscopic electron rotational motion are comparable but not

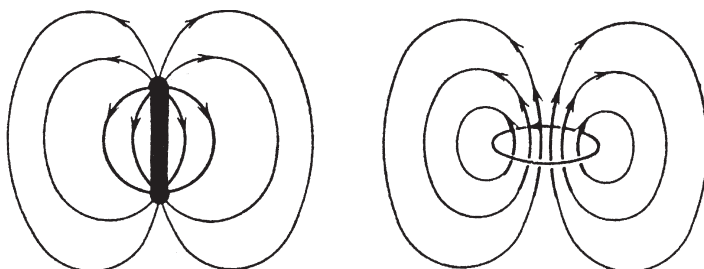


Figure 1.1 Magnetic fields due to a bar magnet and a circuital current.

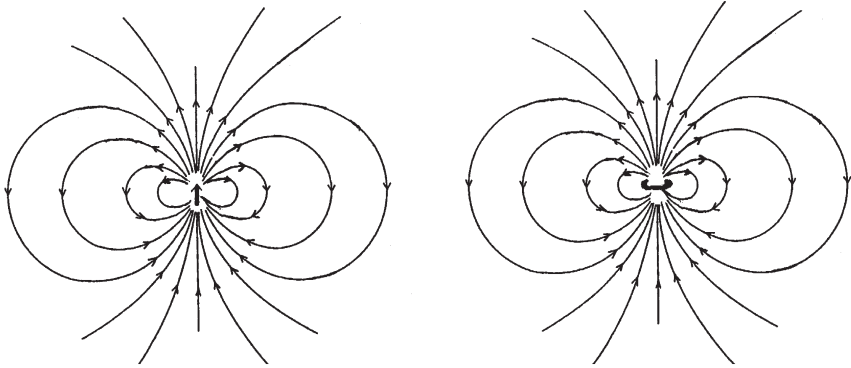


Figure 1.2 Magnetic fields due to a magnetic moment and a small circular current.

discriminated at all. The true understanding of the origin of magnetism, however, has come with quantum mechanics, newly born in the twentieth century.

Before the birth of quantum mechanics vast amounts of data concerning the magnetic properties of materials were accumulated, and a thoroughly logical classification was achieved by observing the response of every material to a magnetic field. These experiments were undertaken using magnetic balances invented by Gouy and Faraday. The principle of magnetic measurement is depicted in Figure 1.3, in which the balance measures the force exerted on the materials in a magnetic field. In general, all materials are classified into two categories, diamagnetic and paramagnetic substances, depending on the directions of the force. The former tend to exclude the magnetic field from their interior, thus being expelled effect in the experiments of Figure 1.3. On the other hand, some materials are attracted

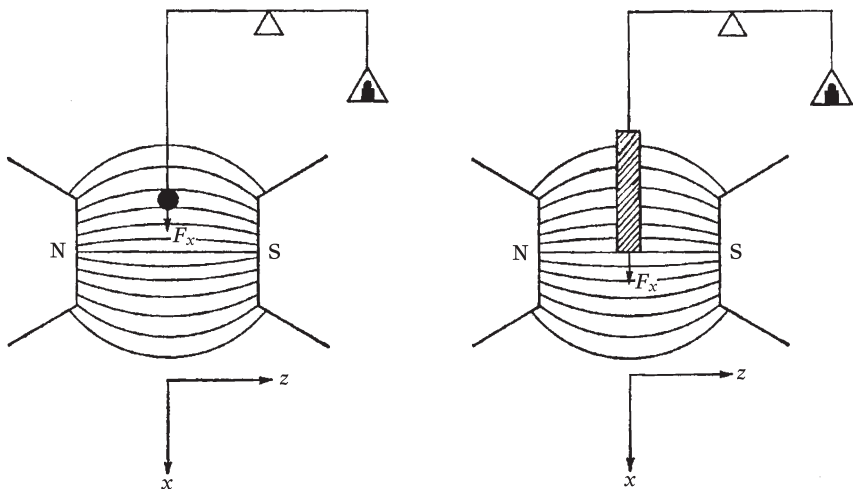


Figure 1.3 Faraday and Gouy balances for magnetic measurements. Force (F_x) is measured.

by the magnetic field. This difference between diamagnetic and paramagnetic substances is caused by the absence or presence of the magnetic moments that some materials possess in atoms, ions, or molecules. Curie made a notable contribution to experiments, and was honored with Curie's law (1895). Our understanding of magnetism was further extended by Weiss, leading to antiferromagnetism and ferromagnetism, which imply different magnetic interactions of magnetic moments with antiparallel and parallel configurations. These characteristics are involved in the Curie–Weiss law. The details will be described one after another in the following sections.

1.1.2

Magnetic Moment and its Energy in a Magnetic Field

The magnetic field generated by an electrical circuit is given as

$$\oint \mathbf{H} \cdot d\mathbf{l} = I \quad (1.1)$$

That is, the total current, I , is equal to the line integral of the magnetic field, \mathbf{H} , around a closed path containing the current. This expression is called “Ampère’s circuital law”. The magnetic field generated by a current loop is equivalent to a magnetic moment placed in the center of the current. The magnetic moment is the moment of the couple exerted on either a bar magnet or a current loop when it is in an applied magnetic field [1]. If a current loop has an area of A and carries a current I , then its magnetic moment is defined as

$$|\mathbf{m}| = IA \quad (1.2)$$

The cgs unit of the magnetic moment is the “emu”, and, in SI units, magnetic moment is measured in Am^2 . The latter unit is equivalent to JT^{-1} . The magnetic field lines around the magnetic moment are shown above in Figure 1.2. In materials the origins of the magnetic moment and its magnetic field are the electrons in atoms and molecules comprising the materials. The response of materials to an external magnetic field is relevant to magnetic energy, as follows:

$$E = -\mathbf{m} \cdot \mathbf{H} \quad (1.3)$$

This expression for energy is in cgs units, and in SI units the magnetic permeability of free space, μ_0 , is added.

$$E = -\mu_0 \mathbf{m} \cdot \mathbf{H} \quad (1.4)$$

This expression in SI units is also represented using the magnetic induction, \mathbf{B} , as defined in the next section. Therefore, the following expression is convenient in SI units:

$$E = -\mathbf{m} \cdot \mathbf{B} \quad (1.5)$$

The SI unit of magnetic induction is T (tesla).

1.1.3

Definitions of Magnetization and Magnetic Susceptibility

Each magnetic moment of a molecular magnet, including atoms or ions, is accounted for as a whole by vector summation. This physical parameter needs a counting base, such as unit volume, unit weight, or, more generally, unit quantity of substance. The last one is the mol (mole), which is widely used in chemistry. This is used in the definition of magnetization, \mathbf{M} , of materials. The units of magnetization, therefore, are emu cm^{-3} , emu g^{-1} , and emu mol^{-1} , or in SI units, A m^{-1} , $\text{A m}^2 \text{kg}^{-1}$, and $\text{A m}^2 \text{mol}^{-1}$, in which A m^2 may be replaced by JT^{-1} .

\mathbf{M} is a property of the material, depending on the individual magnetic moments of its constituent magnetic origins. Considering the vector sum of each magnetic moment, the magnetization reflects the magnetic interaction modes at a microscopic molecular level, resulting in remarkable experimental behaviors with respect to external parameters such as temperature and magnetic field. Magnetic induction, \mathbf{B} , is a response of the material when it is placed in a magnetic field, \mathbf{H} . The general relationship between \mathbf{B} and \mathbf{H} may be complicated, but it is regarded as a consequence of the magnetic field, \mathbf{H} , and the magnetization of the material, \mathbf{M} :

$$\mathbf{B} = \mathbf{H} + 4\pi\mathbf{M} \quad (1.6)$$

This is an expression in cgs units. In SI units the relationship between \mathbf{B} , \mathbf{H} , and \mathbf{M} is given using the permeability of free space, μ_0 , as

$$\mathbf{B} = \mu_0(\mathbf{H} + \mathbf{M}) \quad (1.7)$$

The unit of magnetic induction, in cgs and SI units, is G (gauss) and T (tesla), respectively, and the conversion between them is $1 \text{ G} = 10^{-4} \text{ T}$.

Since the magnetic properties of the materials should be measured as a direct magnetization response to the applied magnetic field, the ratio of \mathbf{M} to \mathbf{H} is important:

$$\chi = \mathbf{M}/\mathbf{H} \quad (1.8)$$

This quantity, χ , is called “magnetic susceptibility”. The magnetization of ordinary materials exhibits a linear function with \mathbf{H} . Strictly speaking, however, magnetization also involves higher terms of \mathbf{H} , and is manifested in the \mathbf{M} vs. \mathbf{H} plot (a magnetization curve). Ordinary weak magnetic substances follow $\mathbf{M} = \chi\mathbf{H}$. The unit of susceptibility is $\text{emu cm}^{-3} \text{Oe}^{-1}$ in cgs units, and because of the equality of $1 \text{ G} = 1 \text{ Oe}$, the unit $\text{emu cm}^{-3} \text{G}^{-1}$ is also allowed. In some literature, especially in

chemistry, χ is given in units of emu mol^{-1} . It should be noted that, in SI units, susceptibility is dimensionless.

The relation between M and H is the susceptibility: the ratio of B to H is called “magnetic permeability”

$$\mu = B/H \quad (1.9)$$

Two equations relating B with H and M (1.6 and 1.7) and the definitions of χ and μ lead to the following relations:

$$\mu = 1 + 4\pi\chi \quad (\text{in cgs units}) \quad (1.10)$$

$$\mu/\mu_0 = 1 + \chi \quad (\text{in SI units}) \quad (1.11)$$

Here, Equation 1.11 indicates the dimensionless relation, and the magnetic permeability of free space, μ_0 , appears again. The permeability of a material measures how permeable the material is to the magnetic field. In the next section the physical explanation will be given after the introduction of magnetic flux.

1.1.4

Diamagnetism and Paramagnetism

Every material shows either positive or negative magnetic susceptibility, that is, $\chi > 0$ or $\chi < 0$. In magnetophysics or magnetochemistry this nature is referred to as “paramagnetism” (displayed by a “paramagnetic material”) in the case of $\chi > 0$ and as “diamagnetism” (displayed by a “diamagnetic material”) in the case of $\chi < 0$. In the M – H curve this behavior is discriminated as a positive or negative slope, as shown in Figure 1.4. Usually, a diamagnetic response toward an external magnetic field is so minor that its slope is very small compared to the paramagnetic case. The difference between paramagnetism and diamagnetism is solely

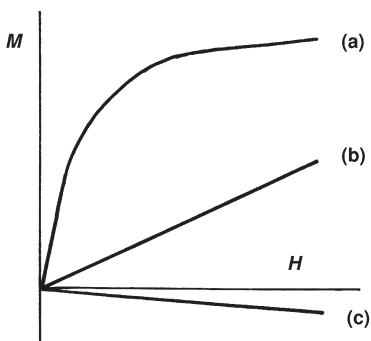


Figure 1.4 Schematic field dependencies of magnetization of (a) ferromagnetic, (b) paramagnetic, and (c) diamagnetic materials.

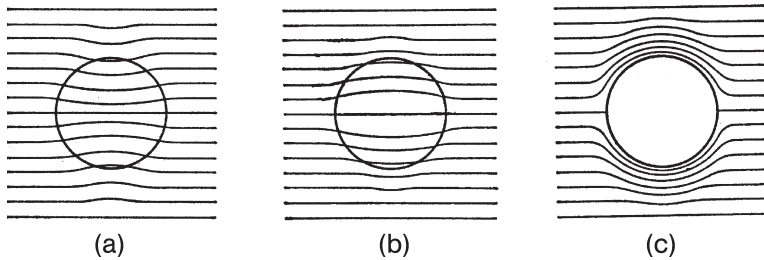


Figure 1.5 Magnetic flux in (a) paramagnetic, (b) diamagnetic, and (c) superconductive materials.

attributed to whether or not the material possesses magnetic moments in atomic, ionic, and molecular states.

Paramagnetic materials sometimes experience magnetic phase transitions at low temperatures. This means cooperative orderings of magnetic moments occur through exchange and dipolar interactions between them. There exist several ordering patterns which specify the vector arrangement of magnetic moments. Ferromagnetic and antiferromagnetic types are typical with parallel and antiparallel orientations, respectively. These magnetisms are called “ferromagnetism” and “antiferromagnetism”. Phenomena concerning the cooperative ordering of magnetic moments are very attractive targets for investigation not only experimentally but also theoretically.

In view of the relationship between χ and μ , positive or the negative magnetic susceptibility corresponds to an increase or decrease in permeability, respectively, in comparison with the applied magnetic field. In order to gain more insight, the concept of “magnetic flux” or “flux density” is discussed here. Magnetic induction, \mathbf{B} , is the same idea as the density of flux, Φ/A , inside the medium, by analogy with $\mathbf{H} = \Phi/A$ in free space. Here, A is the cross-section. This indicates the difference between the external and internal flux, implying the degree of permeability of the magnetic field within a medium. This is illustrated in Figure 1.5, in which the lines indicate the magnetic flux. Perfect diamagnetism, see Figure 1.5c, is specified by $\mathbf{B} = 0$ and is manifested inside superconductors (the “Meissner effect”). From the standpoint of magnetic flux, materials are characterized as “diamagnetic” and either “paramagnetic” or “antiferromagnetic” when magnetic flux inside is less than outside, and the reverse, respectively. In the case of ferromagnetic materials magnetic flux inside is very much greater than that outside. Ferromagnetic materials tend to concentrate magnetic flux within the medium and are characterized by a net overall magnetic moment, which is referred to as “spontaneous magnetization”.

1.1.5

Classification of Magnetic Materials

The basic concept of the magnetic materials is summarized diagrammatically with the help of magnetic moments represented by arrows. No magnetic moment exists

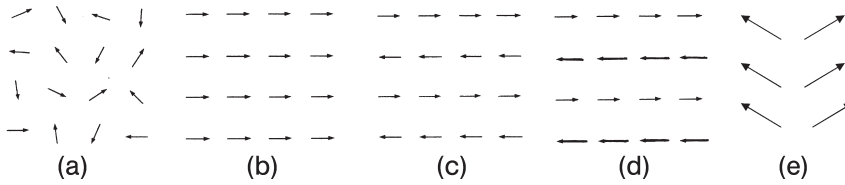


Figure 1.6 Disordered and ordered states of magnetic moments: (a) paramagnetic; (b) ferromagnetic; (c) antiferromagnetic; (d) ferrimagnetic; and (e) canting antiferromagnetic states.

in diamagnetic materials and the magnetic field applied induces a magnetic flux opposite to it. In substances possessing any magnetic moments, each magnetic moment is randomly orientated by thermal agitations, as shown in Figure 1.6a. A decrease of temperature, however, causes magnetic interactions between each magnetic moment to predominate over the thermal energy in the surroundings, thus some ordering of magnetic moments is brought about below the phase transition temperatures. Two typical ordering modes are depicted in Figure 1.6b (a ferromagnetic case) and in Figure 1.6c (an antiferromagnetic case). Materials possessing any magnetic moments respond positively to the magnetic field applied, resulting in both increases of χ and μ .

Here, a comment on the ordering in antiferromagnetism is appropriate. The antiparallel configuration of the magnetic moments has some orientational varieties. One variation concerns a different magnitude in the magnetic moments of each antiferromagnetically interacting pair. This case is termed “ferrimagnetism” (as applied to “ferrimagnetic materials”) and is shown in Figure 1.6d. Such a ferrimagnetic material possesses a net magnetic moment even when the antiparallel array of each moment occurs. Because of this net magnetic moment, although the magnitude itself is far less compared with the ferromagnetic case, the magnetic susceptibility becomes far greater than for a paramagnetic material. The other typical antiparallel arrangement occurs in the case of deviation of co-linearity of magnetic moments (see, Figure 1.6e), which is called “canting antiferromagnetism”. If the canting direction is not countervailed as a whole, then the net magnetic moment survives. Both ferrimagnetism and canting antiferromagnetism are sometimes termed “weak ferromagnetism” on the basis of their spontaneous magnetizations, though these are very small compared to genuine ferromagnetic materials.

1.1.6

Important Variables, Units, and Relations

In consideration of the difference of the unit systems, cgs and SI, the important variables and relations in magnetic study which we have introduced so far are summarized here [1].

	Variables	cgs	SI	Conversion
Energy	E	erg	J (joule)	$1 \text{ erg} = 10^{-7} \text{ J}$
Magnetic field	H	Oe (oersted)	Am^{-1}	$1 \text{ Oe} = 79.58 \text{ Am}^{-1}$
Magnetic induction	B	G (gauss)	T (tesla)	$1 \text{ G} = 10^{-4} \text{ T}$
Magnetic flux	Φ	Mx (maxwell)	Wb (weber)	$1 \text{ Mx} = 10^{-8} \text{ Wb}$
Magnetization	M	emu cm^{-3}	Wb m^{-2}	$1 \text{ emu cm}^{-3} = 12.57 \text{ Wb m}^{-2}$

	Relations	cgs units	Relations	SI units
Magnetic energy	$E = -\mathbf{m} \cdot \mathbf{H}$	erg	$E = -\mu_0 \mathbf{m} \cdot \mathbf{H} = -\mathbf{m} \cdot \mathbf{B}$	J
Magnetic susceptibility	$\chi = M/H$	$\text{emu cm}^{-3} \text{Oe}^{-1}$	$\chi = M/H$	dimensionless
Magnetic permeability	$\mu = B/H$ $= 1 + 4\chi$	GOe^{-1}	$\mu = B/H = \mu_0(1 + \chi)$	$\text{T A}^{-1} \text{m} = \text{H m}^{-1}$

SI units represented by SI fundamental constituents, kg, m, s, and A.

SI symbol	SI unit	Fundamental constituent
N	newton	kg m s^{-2}
J	joule	$\text{kg m}^2 \text{s}^{-2}$
T	tesla	$\text{kg s}^{-2} \text{A}^{-1}$
Wb	weber	$\text{kg m}^2 \text{s}^{-2} \text{A}^{-1}$
H	henry	$\text{kg m}^2 \text{s}^{-2} \text{A}^{-2}$

1.2

Origins of Magnetism

1.2.1

Origins of Diamagnetism

Diamagnetic materials innately possess no magnetic moments in the atoms, ions, or molecules which are their constituents, with the exception that magnetic moments interact with each other most strongly as an “antiparallel pair” so that at ambient temperatures they behave in a diamagnetic ways. Keeping this exception in mind, therefore, a rare origin of diamagnetism is strong twin coupling of magnetic moments in an antiferromagnetic manner. It may be pointed out that, in this case, paramagnetism turns up at an elevated temperature region. Apart

from this exception, what is the general origin of diamagnetism? This may be understood on the basis of Lenz law, which states that, when a magnetic field is applied to a circuit, the current is induced so as to reduce the increased magnetic flux caused by the magnetic field. This means that the circuit is accompanied by a magnetic moment opposite to the applied magnetic field. This is equivalent to the diamagnetism caused by the Larmor precession of electrons. As a simple example we consider a spherical electron distribution around a nucleus and an electron on the sphere at a distance, r (Figure 1.7a).

The electric induction attributed to the applied magnetic field along the z -axis occurs in a plane normal to the magnetic field. The radius, a , of this circuit is related as $a^2 = x^2 + y^2$, where the coordinate of the electron is (x, y, z) . The induced magnetic moment on this loop is expressed in emu using the electron mass, m_e , as

$$\delta m = -(e^2/4m_e c^2) \langle x^2 + y^2 \rangle H \quad (1.12)$$

Here, the symbol $\langle \rangle$ indicates an average in Figure 1.7a. Spherical symmetry assumes $\langle x^2 \rangle = \langle y^2 \rangle = \langle z^2 \rangle = \langle r^2 \rangle / 3$, giving

$$\delta m = -(e^2/6m_e c^2) \langle r^2 \rangle H \quad (1.13)$$

This is summed up for all electrons in the atom, and a molar magnetic susceptibility, χ_M , is given in emu, using the Avogadro constant, N_A , as follows:

$$\chi_M = -(N_A e^2 / 6m_e c^2) \sum \langle r_k^2 \rangle \quad (1.14)$$

This formulae is endorsed by quantum mechanics and the temperature-independency of this value may be understood from the evaluation of $\langle r_k^2 \rangle$ using the wave functions. The energy difference between the wave functions with different

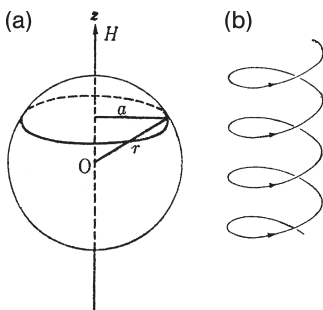


Figure 1.7 (a) Electron rotation in the radius, a ; (b) cyclotron motion caused by the magnetic field.

radial parts is approximates 10 eV. The thermal energy kT at room temperature amounts to approximately 1/40 eV. Thus, diamagnetism exhibits no dependence on temperature. Atomic diamagnetism usually is of the order of $\sim 10^{-6}$ emu, and increases in absolute magnitude for larger atoms with a bigger atomic number because they have a wider radial distribution function.

Diamagnetism for the free electron model is commented on here. It is well known that free electrons are moved by the applied magnetic field, showing a helical motion along the direction of the field. This is called a “cyclotron motion”, which is a counterclockwise circular locus with respect to the magnetic field (see, Figure 1.7b). The frequency of the cyclotron is twice the Larmor frequency and it produces magnetic moments again in opposition to the magnetic field. This magnetic moment is given in emu

$$\delta m = -(ea^2/2c)\omega_c \quad (1.15)$$

where ω_c is the cyclotron frequency and given by $\omega_c = eH/mc$. This is a diamagnetic contribution. However, when these diamagnetic contributions caused by the cyclotron motion are averaged classically for the electron assembly, then macroscopic diamagnetism vanishes. This is the theorem of Miss van Leeuwen. Landau brought this problem to a settlement considering quantization of the helical motions. To cut the matter short, diamagnetic susceptibility is given in emu cm^{-3} as

$$\chi = -(n/2E_F)\mu_B^2 \quad (1.16)$$

Here, n is a density of free electrons and E_F the Fermi energy. The new symbol, μ_B , is called the “Bohr magneton”, which is defined as a unit of magnetic moment. The detail will be described in the following section, referring to the discussion of the origin of paramagnetism.

To summarize this section, diamagnetism is a counteraction of electrons against the magnetic field so as to reduce the increment of magnetic flux caused by the applied field. This is a universal action of electrons. In the presence of magnetic moments originating from electrons such as paramagnetic materials, the opposite action—that is, a cooperative increase of the magnetic flux—takes place very readily, as if a magnetic bar is aligned along the direction of magnetic field. Note that these reactions, diamagnetic and paramagnetic, are combined additively. Now we are ready to comprehend the origins of paramagnetism.

1.2.2

Origins of Paramagnetism

Here we seek the origins of magnetic moments that give rise to paramagnetism. Briefly, magnetic moments are attributable to the angular momenta of the electrons in the atom. The image of the angular momentum of an electron corresponds to Ampère’s circulating circuit, leading to the magnetic moment at the

atomic level, even in the absence of a magnetic field. As we see from the wave functions of the electrons in the hydrogen atom based on the Schrödinger equation and the introduction of the electron spin, there exist two types of angular momenta. One is orbital angular momentum and the other is spin angular momentum. Spin angular momentum is an intrinsic part of an electron itself, regardless of location inside or outside the atom. Finally, the orbital and the spin angular momenta are combined, giving the total angular momentum, which produces the magnetic moments.

The quantum theory of a hydrogen atom is derived from the Schrödinger equation, as follows.

$$\mathcal{H}\Psi = E\Psi$$

$$\mathcal{H} = -\frac{\hbar^2}{2m_e} \left[\frac{1}{r} \frac{\partial^2}{\partial r^2} r + \frac{1}{r^2} \left\{ \frac{1}{\sin^2 \theta} \frac{\partial^2}{\partial \theta^2} + \frac{1}{\sin \theta} \frac{\partial}{\partial \theta} \sin \theta \frac{\partial}{\partial \theta} \right\} \right] - \frac{e^2}{4\pi\epsilon_0 r} \quad (1.17)$$

The first term is the kinetic energy, and the potential energy term, $-(1/4\pi\epsilon_0)(e^2/r)$, is the Coulomb interaction between the electron and the nucleus (proton). As a result of the spherical symmetry of the Coulomb potential, the wave function, Ψ , is separated into the product of the functions of each variable in the spherical coordinates.

$$\Psi_{nlm_l}(r, \theta, \varphi) = R_{nl}(r)\Theta_{lm_l}(\theta)\Phi_{m_l}(\varphi) \quad (1.18)$$

The $R_{nl}(r)$ is called the radial part of the wave function and comprises the associated Laguerre functions. This function contains two types of quantum numbers, n , the principal quantum number and l , the azimuthal quantum number. The angular parts of the spherical coordinates are combined into $Y_{lm_l}(\theta, \varphi) = \Theta_{lm_l}(\theta)\Phi_{m_l}(\varphi)$, which are known as “spherical harmonics”. The angular parts are labeled by two quantum numbers, l and m_l . The latter is named the “magnetic quantum number”, and plays an important role when the magnetic field is applied. The characteristics of the orbital motion of the electron around the nucleus may be described by wave functions with a particular set of quantum numbers, n , l , m_l . These quantum numbers vary under some limitations over integer numbers as

$$\begin{aligned} n &= 1, 2, 3, \dots \\ l &= 0, 1, 2, 3, \dots, (n-1) \\ m_l &= 0, \pm 1, \pm 2, \pm 3, \dots, \pm l \end{aligned} \quad (1.19)$$

The quantum number, l , is replaced by the conventional terminology, s, p, d, . . . , corresponding to $l = 0, 1, 2, \dots$, respectively. These are a natural consequence of physical meanings of the wave function so that the probability of finding an electron in radial and angular motions described by $\Psi_{nlm_l}(r, \theta, \varphi)$ is given by $|\Psi_{nlm_l}(r, \theta, \varphi)|^2$. Thus, the wave function must be a finite, continuous, and one-valued function, and furthermore it is normalized to 1.

The essential point in this situation is that the angular motion which is specified by $Y_l m_l(\theta, \phi)$ is concerned with the orbital angular momentum as long as l is not equal to zero. The magnitude of the orbital angular momentum of an individual electron with the quantum numbers l and m_l is calculated by operating the relevant operators L^2 and Lz for the angular momentum L ,

$$|L| = \sqrt{l(l+1)}\hbar, \quad Lz = m_l \hbar \quad (1.20)$$

From the nature of quantum numbers (1.19), we see that $L \neq 0$ unless $l = 0$. Consequently, the s electrons occupying the s orbitals ($l = 0$) have zero orbital angular momentum, and therefore, no contribution to the magnetic moments. In order to attain an orbital angular momentum pictorially, the case of d -orbitals ($l = 2$) is illustrated in Figure 1.8a, where the five components, $m_l = 2, 1, 0, -1, -2$ are differentiated with respect to the direction of the magnetic field. The magnitude of the orbital angular momentum of the d -orbital is $\sqrt{6}\hbar$ and a little larger than the projected value of the moment to the magnetic field direction. This means that the orbital angular momentum vector can never align along the direction of the magnetic field but makes a precession and forms a cone around the magnetic field direction. This is a quantization image for the angular momentum by the applied magnetic field.

Next we consider the spin angular momentum. For the spin motion of the electron around its own axis, the spin quantum numbers have to be introduced, analogous to the quantum numbers, l and m_l , for the orbital angular momentum.

$$s = 1/2, \quad m_s = \pm 1/2 \quad (1.21)$$

The spin angular momentum, S , and its components are given similarly from the general character of angular momentum

$$|S| = \sqrt{s(s+1)}\hbar = (\sqrt{3}/2)\hbar, \quad Sz = m_s \hbar = (\pm 1/2)\hbar \quad (1.22)$$

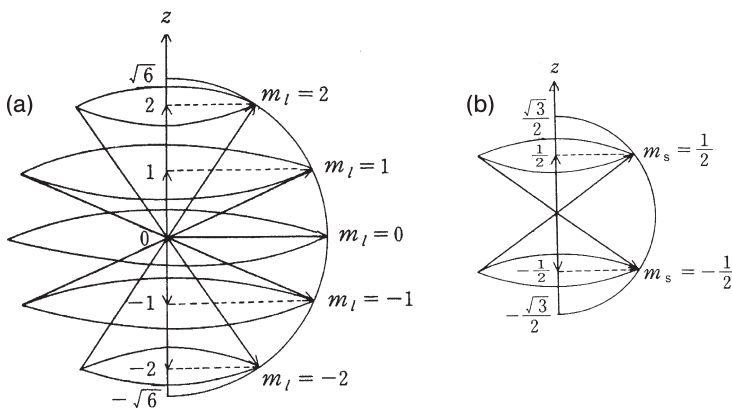


Figure 1.8 Vector model of the quantization of the orbital and spin angular momenta: (a) $l = 2$, (b) $s = 1/2$.

The vector model of the spin angular momentum is also schematically shown in Figure 1.8b. The application of the magnetic field produces two kinds of magnetic moments making precession in a cone. The projection value of the magnetic moments is given by the components of the spin quantum number, m_s , similar to the magnetic quantum number, m_l , of the orbital angular momentum. The spin quantum number is never derived from the Schrödinger Equation 1.17. Taking the relativistic effects into account, Dirac modified the Schrödinger equation, giving rise to the freedom of spin in the electron. Instead of solving the relativistic Dirac equation, we review several experimental matters which led to evidence for the intrinsic presence of electron spin. It was in 1922 that Stern and Gerlach reported to Bohr the atomic beam experiment through the magnetic field gradient, implying that an Ag beam split into two lines when a magnetic field was applied. According to quantum mechanics Ag has no orbital angular momentum. Nevertheless, an Ag atom is classified into two types, one attracted and the other repelled by the magnetic field. This means that even the s electron (5s electron) behaves magnetically and any magnetic moment must be caused by any kind of motion. Thus, two kinds of spin motions, in a clockwise and an anticlockwise manner, were postulated and the angular moment of self-rotations can produce magnetic moments in directions parallel and antiparallel to the magnetic field. The other evidence of the electron spin concerns why the atomic spectrum of Na splits into two D-lines even in the absence of the magnetic field. This phenomenon cannot be explained without “spin” of the electron.

Now we have two kinds of angular momenta in the atom as an origin of the magnetic moment. The orbital and the spin angular momenta are combined vectorially and we define the total angular momentum, using new quantum numbers, j and m_j . In one electron system (l and $s = 1/2$), the total quantum numbers are simple, like $j = l + 1/2$ and $j = l - 1/2$, and m_j is given for each j value as

$$m_j = j, j-1, \dots, -j+1, -j \quad (1.23)$$

From these quantum numbers, the total angular momentum, J , and its components, J_z , is given by

$$|J| = \sqrt{j(j+1)}\hbar, \quad J_z = m_j\hbar \quad (1.24)$$

In this case the state multiplicity is $2j + 1$ and the degeneracy is lifted by the application of the magnetic field, which can explain any Zeeman effect in the materials. The excited state of 3p orbital ($l = 1$) occupied by one electron ($s = 1/2$) for Na is characterized by the quantum numbers, $j = 3/2$ and $1/2$, giving rise to D-line splitting even without the magnetic field.

1.2.3

Magnetic Moments

We have learned that the electrons have two kinds of angular momenta and behave like charged particles forming a loop, giving rise to magnetic moments. Ampère’s

law makes it possible to formulate the relationship between angular momentum and the magnetic moment. Considering the relation of (1.2), $|\mathbf{m}| = IA$, a simple treatment of a circular orbit concludes the magnetic moment relating to the angular momentum, m_l .

$$\begin{aligned} m_z &= -\mu_B m_l \quad (m_l = l, l-1, \dots, -l+1, -l) \\ \mu_B &= e\hbar/2m_e \end{aligned} \quad (1.25)$$

This means that the magnetic moment can be measured in the unit of μ_B , which is called the ‘‘Bohr magneton’’. Note that the magnetic moment vector is opposite to the direction of the angular momentum because of the negative charge of the electron and that this magnetic moment is a projection value to the quantization axis (magnetic field direction). The relationship between the magnetic moment and the angular momentum operator is written as

$$\mathbf{m} = -\mu_B \mathbf{L} \quad (1.26)$$

and the magnitude of the magnetic moment becomes $\mu_B \sqrt{l(l+1)}$.

The magnitude of the Bohr magneton is very important in magnetic science and its value is given in SI units as

$$\mu_B = 9.274 \times 10^{-24} \text{ JT}^{-1} \quad (1.27)$$

In cgs units it is given as

$$\mu_B = e\hbar/2m_e c = 0.927 \times 10^{-20} \text{ erg G}^{-1} \quad (1.28)$$

For the spin angular momentum the deduction of the relationship is not simple because we cannot modify the relation classically but instead resort to the theory of quantum electrodynamics. However, the relation itself seems simple, almost analogous to the orbital angular momentum

$$\mathbf{m} = -g_e \mu_B \mathbf{S}, \quad m_z = -g_e \mu_B m_s, \quad (m_s = 1/2, -1/2) \quad (1.29)$$

in which the newly introduced proportional constant g_e , which is called the g -factor of the electron, is given to be $g_e = 2.002319$ after the relativistic correction. Otherwise $g_e = 2$ is frequently used. Considering the spin quantum numbers are $s = 1/2$ and $m_s = \pm 1/2$, the magnetic moment of the electron is counted as one Bohr magneton.

In summary, the combined magnetic moments are given as a result of the two contributions from each angular momentum, as follows:

$$\mathbf{m} = -\mu_B (\mathbf{L} + g_e \mathbf{S}) \quad (1.30)$$

In this section it is instructive also to describe the nuclear magnetic moment in comparison with the above-mentioned electron case. The nuclear magnetic

moment originating from the nuclear spin quantum number, I , is given by a similar relation to (1.29) for the electron spin as follows:

$$\mathbf{m}_n = g_n \mu_n \mathbf{I}, \quad m_{nz} = g_n \mu_n m_l, \quad (m_l = I, I-1, \dots, -I+1, -I) \quad (1.31)$$

Here, \mathbf{I} is a nuclear spin operator and g_n is a proportionality constant called the “nuclear g -value”. Each nucleus possesses its original I and g_n -value. The nuclear Bohr magneton, μ_n , is a unit of the nuclear magnet and is defined in SI units, analogous to the Bohr magneton (1.25), by

$$\mu_n = e\hbar/2m_p = 5.05824 \times 10^{-27} \text{ JT}^{-1}. \quad (1.32)$$

Here m_p represents a mass of proton. Therefore, the ratio of $|\mu_B/\mu_n|$, which is equal to m_p/m_e , is in the order of 10^3 , indicating the dominant contribution of the electron to the magnetic moments of materials and the far stronger magnetic interactions between the electron magnetic moments. For ^1H (proton) $I = 1/2$ and $g_n = 5.585$, yielding $m_n = 2.7927 \mu_n$. ^{14}N with $I = 1$ possesses $m_n = 0.4036 \mu_n$. Finally, it may be understood that the relations (1.31) have a positive sign, differing from the electron case with a negative sign, owing to the positive charge of the nucleus.

1.2.4

Specific Rules for Many Electrons

In general atoms or ions there exist many electrons (except the hydrogen-like atoms) so we have to take into account additional rules concerning electron configurations; these are called the “Aufbau principle”. It is easy to understand that electrons occupy wave functions with lower energy first. The second rule tells us that double occupation with the same quantum numbers (n, l, m_l, m_s) is prohibited; this is the well-known “Pauli exclusion principle”. Because the orbital wave function is designated by (n, l, m_l), a maximum of two electrons can occupy each orbital wave function and their spin quantum numbers $m_s = \pm 1/2$ should be different. This means that an electron is likely to make a pair with the opposite spin. In the occupation process we need an additional law for the degenerate orbitals such as $l \neq 0$. This is “Hund’s rule”. First, the electrons maximize their total spin, which is realized when each electron occupies an individual orbital separately with parallel spins. After the one-electron occupations are completed within the degenerate orbitals, antiparallel spins start to reside. Second, for a given spin arrangement the electron configuration for the lowest energy results in the largest total orbital angular momentum.

For a many-electron atom we have to consider the orbit–orbit, spin–orbit, and spin–spin interactions between the angular momenta of the individual electron specified by the quantum numbers, l and s . The orbital angular momentum induces a magnetic moment at the nucleus, and hence exerts a magnetic field at the electron, which interacts with an electron magnetic moment originated from

its spin. This magnetic interaction mechanism is called the spin–orbit coupling, which is the most important interaction in magnetism and magnetic resonance because it actually couples between the orbital wave functions and electron spins. The magnitude of the spin–orbit coupling is determined by presuming the orbiting motion of the nucleus around the electron specified by the electron wave function. Therefore, spin–orbit interaction is proportional to the nuclear charge and thus nuclear number, Z , as is expressed by the Hamiltonian between the orbital and spin operators, \mathbf{l}_i and \mathbf{s}_i for an i electron

$$\mathcal{H} = \zeta \mathbf{l}_i \cdot \mathbf{s}_i, \quad \zeta = 2Z\mu_B^2 \langle 1/r^3 \rangle \quad (1.33)$$

where $\langle 1/r^3 \rangle$ means an orbital average. For many-electron cases this coupling has to be summed up. In this process, when the spin–orbit coupling is weak for the light atoms, the couplings between the individual orbital angular momenta and the individual spin angular momenta become predominant. Consequently, the summation of (1.33) is transformed into the next Hamiltonian as a result of $\mathbf{L} = \sum \mathbf{l}_i$ and $\mathbf{S} = \sum \mathbf{s}_i$.

$$\mathcal{H} = \lambda \mathbf{L} \cdot \mathbf{S} \quad (1.34)$$

This is an important Hamiltonian called the spin–orbit coupling. In summing up the individual orbital and spin angular momenta, special rules are concluded for the characteristic configurations of electrons in a certain shell. For a fully filled shell, \mathbf{L} and \mathbf{S} , therefore the spin–orbit coupling vanishes. Besides, a half-filled shell gives $L = 0$ and $S = (2l + 1)/2$; again, no spin–orbit interaction. We classify the remaining configurations by “less than half” and “more than half”. The coefficient λ of the shell-electron number, n , is given as $\lambda = \zeta/n$ for the former case and as $\lambda = -\zeta/(4l + 2 - n)$ for the latter case, and a positive or negative λ is deduced for the “less than half” or “more than half” configurations, respectively. For example, therefore, a “less than half” atom is likely to couple the total orbital and total spin momenta with an antiparallel configuration

Next we proceed to Russell–Saunders coupling. As we see from the above discussion, a weak spin–orbit coupling is assumed in this derivation. The allowed values of the added angular momenta are explained for simplicity in the two-electron case, the orbital quantum numbers, l_1 and l_2 and the spin quantum numbers, s_1 and s_2 . The allowed total orbital and spin quantum numbers are as follows:

$$L = l_1 + l_2, l_1 + l_2 - 1, \dots, |l_1 - l_2|, \quad S = s_1 + s_2, s_1 - s_2 \quad (1.35)$$

Actually $s_1 = s_2 = 1/2$, then we obtain $S = 1$ and $S = 0$. This method is repeated for more than three electrons. The components of the combined angular momenta are specified using m_L and m_S , analogous to the m_l and m_s , as follows:

$$m_L = L, L - 1, \dots, -L, \quad m_S = S, S - 1, \dots, -S \quad (1.36)$$

The values $2L + 1$ or $2S + 1$ are the number of the components which belong to L or S quantum numbers, respectively. These are called the “orbital multiplicity” and the “spin multiplicity” indicating the number of the degenerate states in free atoms. The corresponding angular momenta are given using these quantum numbers as

$$\begin{aligned} |L| &= \sqrt{L(L+1)}\hbar, & L_z &= m_l \hbar \\ |S| &= \sqrt{S(S+1)}\hbar, & S_z &= m_s \hbar \end{aligned} \quad (1.37)$$

The total angular momentum is then determined by the same vector summation of the total orbital and spin angular momenta.

$$J = L + S, L + S - 1, \dots, |L - S|, \quad m_J = J, J - 1, \dots, -J \quad (1.38)$$

The multiplicity is $2J + 1$, and the magnitudes of the total angular momentum are

$$|J| = \sqrt{J(J+1)}\hbar, \quad J_z = m_J \hbar \quad (1.39)$$

Now the description of the atomic state can be characterized using the three angular momenta, L , S , and J , and their quantum numbers, L , S , and J . In general, the atomic or its ionic states are specified by the atomic “term”, like ${}^2P_{3/2}$ or ${}^2P_{1/2}$ for 3p-excited Na. The central capital alphabets, S, P, D, F, , , mean $L = 0, 1, 2, 3, \dots$, respectively, and the superscript indicates the multiplicity of $2S + 1$ and the subscript J quantum numbers. Incidentally, the Na ground state is represented by ${}^2S_{1/2}$ and its excited states by a lower ${}^2P_{1/2}$ and a higher ${}^2P_{3/2}$. This is the origin of the two D-lines.

In closing this section, we remark on the case in which the Russell–Saunders coupling fails. For the heavier atoms the spin–orbit coupling becomes so strong that, in atoms such as the actinides like U, the spin and orbital angular momenta of the individual electrons couple first, and then the combined quantum number, $j_i = l_i + s_i$, becomes a good quantum number. The resultant angular momentum, j_i , interacts with another, giving the total angular momentum,

$$j_i = l_i + s_i, \quad J = \sum j_i \quad (1.40)$$

This is the j – j coupling and the quantum numbers, L and S , are meaningless. Nevertheless, the Russell–Saunders coupling can be applied effectively even for the rare earth elements (lanthanoids). Usually, therefore, there is no need to take account of the j – j coupling.

1.2.5

Magnetic Moments in General Cases

As we summarized above, in Section 1.2.3, the combined magnetic moment is given by 1.30. This relation is derived for one electron having l and s quantum

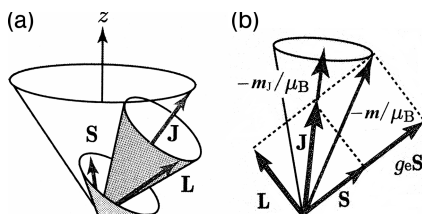


Figure 1.9 (a) Angular momenta, L , S , and J , and (b) magnetic moments, m and m_j , related with L , S , and J .

numbers. For many electrons this is also the case in which the meanings, L and S , are modified as the operators referring to the combined orbital and spin angular momentum, $L = \Sigma l_i$ and $S = \Sigma s_i$. In the case of the effective Russell–Saunders coupling, the total quantum number, J , as a result of the combined contribution between the total orbital and spin angular momenta, becomes a good quantum number. This means that the two physically significant parameters, the magnetic moment, m , and the total angular momentum, J , are not collinear. This situation is depicted in Figure 1.9, assuming $g_e = 2$. The projected magnitude of the magnetic moment, m , along the J axis is given as a following relation of the total angular momentum operator, J .

$$\mathbf{m}_j = -g_j \mu_B \mathbf{J} \quad (1.41)$$

$$g_j = 1 + \frac{J(J+1) + S(S+1) - L(L+1)}{2J(J+1)}$$

Here, g_j is called the Landè g -factor. The magnitude of the total magnetic moment and its component are given as follows

$$|\mathbf{m}_j| = g_j \mu_B \sqrt{J(J+1)}, \quad m_{jz} = g_j \mu_B m_j \quad (1.42)$$

where $m_j = J, J-1, \dots, -J$. The special important cases are $S = 0$ or $L = 0$, that is, either contribution of the orbital or the spin angular momentum to the magnetic moment. Then the above equation implies $g_j = 1$ for $S = 0$ and $g_j = 2$ for $L = 0$. The latter case is “spin only” contribution to the magnetic moment,

$$|\mathbf{m}_s| = g_e \mu_B \sqrt{S(S+1)}, \quad m_{sz} = g_e \mu_B m_s \quad (1.43)$$

where $m_s = S, S-1, \dots, -S$.

1.2.6

Zeeman Effect

The Zeeman effect was observed in the spectroscopy of the emitted light from the atoms under the influence of the magnetic field. Compared to the atomic spectra without the magnetic field, the additional splittings of the spectra were detected,

which are ascribed to the interaction of the atomic magnetic moments with the magnetic field. The energy of this interaction is given, in cgs units, by

$$E = -\mathbf{m} \cdot \mathbf{H} \quad (1.44)$$

In SI units this relation is modified by μ_0 as $E = -\mu_0 \mathbf{m} \cdot \mathbf{H}$, thus,

$$E = -\mathbf{m} \cdot \mathbf{B} \quad (1.45)$$

Replacing \mathbf{m} with the angular momentum operator, \mathbf{J} , the Hamiltonian becomes

$$\mathcal{H} = g_J \mu_B \mathbf{J} \cdot \mathbf{H}, \quad \mathcal{H} = g_J \mu_B \mathbf{J} \cdot \mathbf{B} \quad (1.46)$$

This is called the “Zeeman Hamiltonian” (the Zeeman term) or the “Zeeman energy”. From these energy representations, it is clear that the Zeeman energy depends not only on the quantum number, J , but also on the quantum numbers, L and S , because g_J includes L , S , and J . In “spin only” case, it is given by

$$\mathcal{H} = g_s \mu_B \mathbf{S} \cdot \mathbf{H}, \quad \mathcal{H} = g_s \mu_B \mathbf{S} \cdot \mathbf{B} \quad (1.47)$$

Considering the components of J , the Zeeman splitting can be explained. For example, the D-lines of Na are observed as ${}^2P_{3/2} \leftrightarrow {}^2S_{1/2}$ and ${}^2P_{1/2} \leftrightarrow {}^2S_{1/2}$. Under the application of the external magnetic field the line number increases depending on each component of the sublevels. Historically, the Zeeman effects were discriminated as the normal and anomalous Zeeman effects. The reason of this situation is attributable to incomplete understanding in the periods of no idea of the electron spin. The “anomalous” term is no more anomalous after the introduction of the assured existence of the electron spin and hence of the spin-orbit coupling.

1.2.7

Orbital Quenching

The expectation value of the orbital angular momentum, L , for a certain orbital, Ψ , is obtained from the integral, $\langle L \rangle = \hbar \int \Psi^* \mathbf{L} \Psi d\tau$. Here \mathbf{L} is the operator of the orbital angular momentum. The quenching of the orbital angular momentum means $\langle L \rangle = 0$, that is, the expectation value of any component of the orbital angular momentum vanishes. Under what circumstances is the angular momentum quenched? Let us see how it comes for L_z , which is represented as $L_z = (1/i)(x\partial/\partial y - y\partial/\partial x) = (1/i)(\partial/\partial\phi)$. The important point is that L_z is a pure imaginary operator (this is also the case for the other components). In addition, the operator, L_z , is a “Hermitian operator”, so the diagonal element must be real. As long as the wave function, Ψ , is real, the matrix element must be zero from the requirement of “Hermiticity”. This is called the “orbital quenching”. The real wave function can be brought about when the electronic orbital motion interacts strongly

with the crystalline electric fields. This has something to do with the lifting of the degenerate orbital energies. Non-degenerate atomic or molecular orbitals must be real. This theorem is easily comprehensible if one considers that, for an assumed complex wave function, the complex conjugate of the wave function also satisfies the original Schrödinger equation with a same eigenvalue. We conclude that the crystal field produced by a symmetric environment can, at least partially, quench the orbital angular momentum of the atom. In this situation, $\mathcal{H} = \lambda \mathbf{L} \cdot \mathbf{S}$ should be treated as a perturbation for the discussion of the spin system. In the complete quenching cases, the quantum number, J , and its operator, \mathbf{J} , can be replaced by the quantum number, S , and its operator, \mathbf{S} , respectively, in concert with the replacement of g_l with g_e and, therefore, the magnetic moment includes only spin origin, $\mathbf{m} = -g_e \mu_B \mathbf{S}$. The partial or incomplete quenching implies remaining orbital angular momentum to some extent, resulting in some contribution of the orbital angular momentum to the magnetic moments. In the perturbation of $\lambda \mathbf{L} \cdot \mathbf{S}$, the g -factor deviates from g_e , the magnetic moment being $\mathbf{m} = -g \mu_B \mathbf{S}$. In this context observation of the g -value in the electron spin resonance (ESR), spectroscopy is of considerable significance.

As an example of orbital quenching, the magnetic data are summarized for the transition metal ions in comparison with the data of the rare-earth ions (Table 1.1). The experimental magnetic moment, \mathbf{m} , is listed in the unit of μ_B and the theoretically estimated values correspond to the quenching and non-quenching cases based on the formulae, $g_e \sqrt{S(S+1)}$ and $g_l \sqrt{J(J+1)}$. The data of the transition ions are in good agreement with the value, $g_e \sqrt{S(S+1)}$, rather than the data from the total angular momentum, J . This means almost complete quenching of the orbital angular momentum, and accordingly the magnetic origin is exclusively attributed to spin, so that this is a so-called “spin only” case or magnetism. In some examples, such as Fe^{2+} , Co^{2+} , or Ni^{2+} , a little deviation is noticeable. These belong to the incomplete or partial quenching case and sometimes the orbital wave

Table 1.1 Magnetic moments of $3d^n$ and $4f^n$ ions.

n	Ions	μ/μ_B	S	J
1	$\text{Ti}^{3+}, \text{V}^{4+}$	1.8	1.73	1.55
2	V^{3+}	2.8	2.83	1.63
3	$\text{V}^{2+}, \text{Cr}^{3+}$	3.8	3.87	0.77
4	$\text{Cr}^{2+}, \text{Mn}^{3+}$	4.9	4.90	0
5	$\text{Mn}^{2+}, \text{Fe}^{3+}$	5.9	5.92	5.92
6	Fe^{2+}	5.4	4.90	6.70
7	Co^{2+}	4.8	3.87	6.63
8	Ni^{2+}	3.2	2.83	5.59
9	Cu^{2+}	1.9	1.73	3.55
10	Zn^{2+}	0	0	0

$$S = 2\sqrt{S(S+1)}, \quad J = g_l \sqrt{J(J+1)}$$

functions are nearly degenerate. Consequently, remarkable g -factors apart from the free electron, g_e , and its anisotropy are observed for these materials. For the $4f^n$ ions from Ce^{3+} and Yb^{3+} , on the other hand, the agreement between the experiment and the theory is considered good except Eu^{3+} . The rare-earth ions containing f -electrons as an origin of magnetism are good examples for the Russell–Saunders coupling. The exceptional discrepancy in the data of Eu^{3+} is explained that the quantum numbers are $L = 3$, $S = 3$, and $J = 0\sim 6$ in the Russell–Saunders category, and $3.4\mu_B$ is due to the excited states above the ground 7F_0 ($J = 0$) populated at room temperature.

1.3 Temperature Dependence of Magnetic Susceptibility

1.3.1

The Langevin Function of Magnetization and the Curie Law

We discuss an ensemble of non-interacting magnetic moments with the same origin in the applied field, \mathbf{H} , at the temperature, T . The probability of occupying an energy state, $E = -\mathbf{m}\cdot\mathbf{H}$, is given by Boltzmann statistics, that is, $\exp(-E/kT) = \exp(mH\cos\theta/kT)$, where θ is an angle of the magnetic moment, \mathbf{m} , to the applied field, \mathbf{H} , and m and H indicate the magnitude of each vector. One has to know the number of the magnetic moments lying between the angles, θ and $\theta + d\theta$, with respect to the magnetic field. Its probability, $P(\theta)$, is related to the fractional area, dA , of the surface of the sphere covering the angles between θ and $\theta + d\theta$ at a constant radius, r . In view of $dA = 2\pi r^2 \sin\theta d\theta$, the overall probability, including the above-mentioned Boltzmann factor, is given by

$$P(\theta) = \frac{e^{mH\cos\theta/kT} \sin\theta d\theta}{\int_0^\pi e^{mH\cos\theta/kT} \sin\theta d\theta} \quad (1.48)$$

The magnetization, \mathbf{M} , parallel to the applied field is a total vector sum of each component, $\mathbf{m}\cos\theta$, and therefore, the magnetization of the whole system amounts to

$$\mathbf{M} = N\mathbf{m} \frac{\int_0^\pi e^{mH\cos\theta/kT} \cos\theta \sin\theta d\theta}{\int_0^\pi e^{mH\cos\theta/kT} \sin\theta d\theta} \quad (1.49)$$

Here, N is the number of the magnetic moment, \mathbf{m} , in the whole system. This equation can be represented by the following formulae after the integrals are carried out mathematically.

$$\mathbf{M} = N\mathbf{m}[\coth(mH/kT) - kT/mH] = N\mathbf{m}L(\alpha) \quad (1.50)$$

The function $L(\alpha) = \coth(\alpha) - 1/\alpha$ as a function of $\alpha = mH/kT$, is called the "Langevin function", which is shown in Figure 1.10. We check the features of the

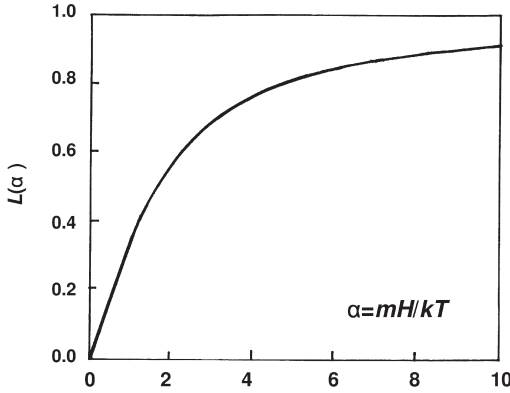


Figure 1.10 The Langevin function $L(\alpha)$, expressed in M/Nm vers. $\alpha = mH/kT$.

Langevin function in the specific areas of $\alpha \gg 1$ and $\alpha \ll 1$. For $\alpha \gg 1$ this is the case either in a very large magnetic field, H , or at very low temperature, T , near zero kelvin. Then $L(\alpha) \rightarrow 1$, and M approaches Nm . The largest value, $M = Nm$, is equivalent to the complete alignment of the magnetic moments along the magnetic field, H . What about $\alpha \ll 1$, which may be achieved by the opposite parameters setting to the $\alpha \gg 1$? In this case the Langevin function can be expanded as a Taylor series. Keeping only the prominent term, we have

$$M = Nm^2(H/3kT) \quad (1.51)$$

This relation indicates that the magnetization is proportional to the applied field and inversely proportional to the temperature. Thus, the magnetic susceptibility $\chi = M/H$ is obtained as

$$\chi = C/T, \quad C = Nm^2/3kT \quad (1.52)$$

This relation was experimentally obtained by Curie, and is called the ‘‘Curie law’’, where the constant, C , is a Curie constant. In conclusion, the magnetic susceptibility of paramagnetic materials without particular magnetic interactions obeys this law, and the characteristics of this behavior are ascertained by a simple formula; that is, an inverse proportionality to the temperature.

1.3.2

The Brillouin Function of Magnetization and the Curie Law

As we have discussed, each magnetic moment is expressed by $\mathbf{m} = -g_j\mu_B \mathbf{J}$, and its Zeeman energy is $E = g_j\mu_B \mathbf{J} \cdot \mathbf{H} = g_j\mu_B m_j H$, where m_j takes $J, J-1, \dots, -J$. Thus, we calculate $\langle m_j \rangle$ instead of $\langle \cos\theta \rangle$ by replacing the integral in the average with Σ of m_j . Eventually we obtain the Brillouin function, $B_J(\alpha)$.

$$M = Ng_j \mu_B J \left\{ \frac{2J+1}{2J} \coth \frac{2J+1}{2J} \alpha - \frac{1}{2J} \coth \frac{1}{2J} \alpha \right\} = Ng_j \mu_B J B_J(\alpha) \quad (1.53)$$

The function $B_J(\alpha) = \{(2J + 1)/2J\} \coth\{(2J + 1)/2J\} \alpha - (1/2J) \coth \alpha / 2J$ is called the “Brillouin function” as a function of $\alpha = g_j \mu_B JH/kT$, which is equal to the Lengevin function in the limit of $J \rightarrow \infty$. The Brillouin functions for some typical quantum numbers are depicted in comparison with the experimental data (Figure 1.11) [2], where the transition ions, Fe^{3+} and Cr^{3+} , are the case of the orbital quenching (see Table 1.1) so that J should be replaced by S in the Brillouin function, and the data for Gd^{3+} is also the case of $L = 0$, therefore $J = S = 7/2$, $g_j = 2$. We examine the specific areas of $\alpha \gg 1$ and $\alpha \ll 1$. These conditions are expected in a similar manner regarding the parameters, H and T . In the conditions of $\alpha \gg 1$, we get $B_J(\alpha) \rightarrow 1$. Consequently, the magnetization approaches $M = Ng_j \mu_B J$, the saturated values in Figure 1.11. For $\alpha \ll 1$ the Brillouin function can be also expanded in a Taylor series. Keeping the first meaningful term, the magnetic susceptibility is represented by the Curie law, similar in form to the Lengevin case:

$$\chi = C/T, \quad C = Ng_j^2 \mu_B^2 J(J+1)/3k \quad (1.54)$$

Comparing the two derived forms of the Curie law from the Langiven and the Brillouin functions, one sees that the Curie constant sheds light on the quantum mechanical meaning of the microscopic magnetic moment, that is,

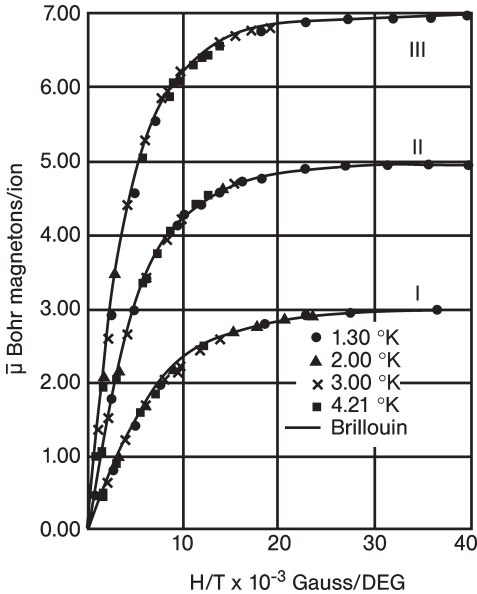


Figure 1.11 Brillouin function for $J = 3/2$ (I), $J = 5/2$ (II), and $J = 7/2$ (III) and magnetic data of Cr^{3+} ($S = 3/2$), Fe^{3+} ($S = 5/2$), and Gd^{3+} ($S = 7/2$).

$$\mathbf{m}^2 = g_J^2 \mu_B^2 J(J+1) \quad (1.55)$$

This is the previous conclusion from the operator representation of \mathbf{m}_J (1.41) and its magnitude (1.42). In this context the effective Bohr magneton, m_{eff} , is defined as

$$m_{\text{eff}} = g_J \mu_B \sqrt{J(J+1)} \quad (1.56)$$

Again, in the case of orbital quenching, m_{eff} is equal to $g_e \mu_B \sqrt{S(S+1)}$. Finally, it may be added that the magnetic susceptibility, χ , in SI units should be multiplied by μ_0 in the Curie law, and, thus, the Curie constant becomes $\mu_0 N g_J^2 \mu_B^2 J(J+1)/3k$.

1.3.3

The Curie–Weiss Law

In reality the observed magnetic susceptibilities do not obey the Curie law. This is because, in the above derivation of the Curie law, we have assumed isolated magnetic moments and thus no magnetic interactions are included. Many magnetic materials possess various magnetic interactions, more or less, between the individual magnetic moments, leading to the Curie–Weiss law

$$\chi = C/(T - \theta) \quad (1.57)$$

where the correction term, θ , has the unit of temperature, and is called the “Weiss constant”, which is empirically evaluated from a plot of $1/\chi$ vs T . These techniques are shown schematically in Figure 1.12 in comparison with the Curie law. The intercepts of the data with the abscissa take place away from the origin, whereas the straight line crosses at the origin for the Curie law. Here we derive the Curie–Weiss law on the assumption of the existence of magnetic interactions. Although Weiss did not explain the details of the interactions between the mag-

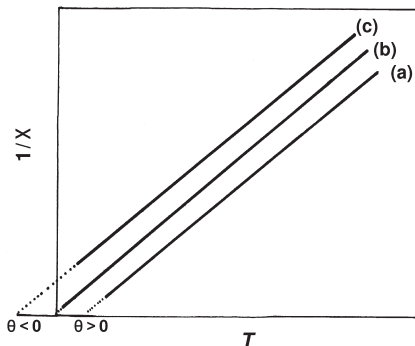


Figure 1.12 Curie–Weiss laws with (a) $\theta > 0$ and (c) $\theta < 0$ compared with (b) Curie law.

netic moments, the fundamental concept is “a molecular field” arising from the magnetization and acting on the magnetic moments in addition to the external magnetic field. The molecular field is directly proportional to the magnetization, M , and the effective magnetic field, H_{eff} , is expressed as combined with the applied magnetic field, H .

$$H_{\text{eff}} = H + \Gamma M \quad (1.58)$$

Where a term, ΓM , is a molecular field and Γ is called the “molecular field coefficient”. In the Curie law relation $M/H = C/T$, and H_{eff} of (1.58) is inserted into this magnetic field, H , then we have the following relation:

$$M = CH/(T - C\Gamma) \quad (1.59)$$

In the expression of $\chi = M/H$, the Curie–Weiss law is obtained with the Weiss constant, $\theta = C\Gamma$. The Curie–Weiss law predicts anomalous behaviors at the temperature, $T_C = \theta$. The divergence of the magnetic susceptibility corresponds to the phase transition to the spontaneously magnetic ordered phase. The phase transition temperature is called the “Curie temperature” (T_C). Below this temperature, the material exhibits ferromagnetism with a spontaneous magnetization. A positive value of θ indicates that a molecular field is acting in the same direction as an applied field, so the magnetic moments are likely to align in parallel with each other, in the same direction as the magnetic field.

On the other hand, we sometimes observe a negative value of θ , in which the arrangement of the magnetic moment seems opposite, like antiferromagnetism. We see Néel’s interpretation on the antiferromagnetic formalism. In the simplest alignment of magnetic moments, one can presume two sublattices, each of which comprises the same magnetic moments in the same orientation. These structurally identical sublattices are labeled A and B, and have magnetic interactions with each other, A–A, A–B, and B–B. Ignoring the A–A and B–B interactions, the magnetic moments in the A sublattice see the molecular field generated by the magnetic moments in the sublattice B, and vice versa. In comparison with the ferromagnetic case, the molecular field is apparently opposite in direction; thus, we assume

$$H_{\text{eff}}^A = H - \Gamma M_B, \quad H_{\text{eff}}^B = H - \Gamma M_A \quad (1.60)$$

Here, M_A and M_B are the magnetizations of the sublattices A and B, respectively. Following the same procedure in the ferromagnetic case, we have the sublattice magnetizations, M_A and M_B .

$$M_A = C'(H - \Gamma M_B)/T, \quad M_B = C'(H - \Gamma M_A)/T \quad (1.61)$$

The total magnetization, M , is given by $M = M_A + M_B$, resulting in

$$\mathbf{M} = 2C'\mathbf{H}/(T + C\Gamma) \quad (1.62)$$

In the expression of $\chi = M/H$, the Curie–Weiss law is obtained with the negative Weiss constant, $\theta = -C\Gamma$. The Curie–Weiss law predicts anomalous behavior at the temperature, $T_N = -\theta$. Although the divergence of the magnetic susceptibility, like a ferromagnetic case, is not concomitant, the phase transition from a paramagnetic to an antiferromagnetic state takes place. In the antiferromagnetic ordered state each sublattice is spontaneously magnetized just like the spontaneous magnetization of the ferromagnets. This phase transition temperature is called the “Nèel temperature” (T_N).

In conclusion, the Curie–Weiss law is compatible with the existence of ferromagnets and antiferromagnets. The characteristics of the magnetic ordered states have to be described more, and the mechanisms of the interactions of the magnetic moments must be scrutinized for further comprehension of the magnetism from a quantum mechanical point of view. This is a physical research subject on magnetic cooperative phenomena.

1.3.4

Magnetic Ordered State

We focus our attention to how the magnetic ordered states come out. According to the Curie–Weiss law, magnetic susceptibility at temperatures crossing the phase transition, T_C , is discontinuous and it diverges at $T = T_C$, then what happens in between the paramagnetic and ferromagnetic phase transition? Let’s consider again the Brillouin function as a function of $\alpha = g_j\mu_B JH/kT$. In the Weiss molecular field, the external magnetic field, H , is replaced by H_{eff} , including $\Gamma M(T)$. In the absence of the external magnetic field, H , the following two relations are worked out:

$$M(T)/M(0) = B_j(\alpha), \quad M(T)/M(0) = (kT/Ng_j^2\mu_B^2J)\alpha \quad (1.63)$$

Here, $M(0) = Ng_j\mu_B J$ is the maximum magnetization at $T = 0$. The Brillouin function varies as a function of α , as is shown above in Figure 1.11, whereas the latter is a linear function of α . The significant physical solutions are those where the two curves intersect. The unquestioned solution that occurs at the origin is devoid of meaning. Lowering the temperature the slope of the linear function gradually decreases, so that we have another intersection in addition to the origin, revealing the presence of the spontaneous magnetization. Figure 1.13 illustrates this mathematical meaning in three temperature regions, $T > T_C$, $T = T_C$, and $T < T_C$. It is essential that, at T_C , the linear function is a tangent line to the Brillouin function, and that, below T_C , spontaneous magnetization starts to grow. The spontaneous magnetization, $M(T)/M(0)$ is plotted in Figure 1.14 as a function of T/T_C for $J = 1/2$, $J = 1$, and $J = \infty$.

It is added as a summary that, in the approximation of the Weiss molecular field, the Curie temperature, T_C , is expressed with $m_{\text{eff}} = g_j\mu_B\sqrt{J(J+1)}$ as

$$T_c = Nm_{\text{eff}}^2 \Gamma / 3k \tag{1.64}$$

This relation reveals that the larger the quantum number, J , and molecular field coefficient, Γ , the higher T_c is expected to be implying the large magnetic moments and the strong interactions between them are effective to obtain ferromagnetic materials at high temperatures.

Here we describe the distinguishable response of ferromagnetic materials: it is a magnetization curve under a magnetic field cycle in which, after the magnetic field is applied to reach a certain high value, the field is reduced to zero, and then it is reversed in direction, making a loop. The magnetization, M , is traced out versus H , as shown in Figure 1.15, and is called a “hysteresis curve”. The initial increase of the magnetization starts at the origin (the unmagnetized state), O , and it reaches a maximum value (the “saturation magnetization”), $M_s = N g \mu_B J$. In the reducing process of the field the magnetization does not conform to the origi-

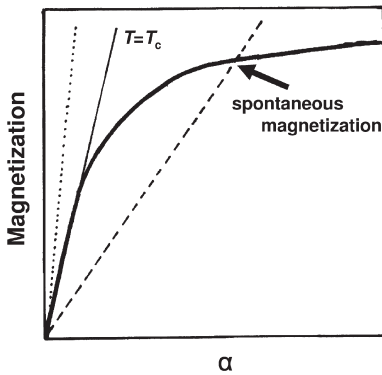


Figure 1.13 Graphical illustration of Brillouin function and spontaneous magnetization. At $T > T_c$ the dotted line crosses only at the origin ($\alpha = 0$) and at $T < T_c$ the dashed line hits at $\alpha \neq 0$. At $T = T_c$ a solid line becomes a tangent.

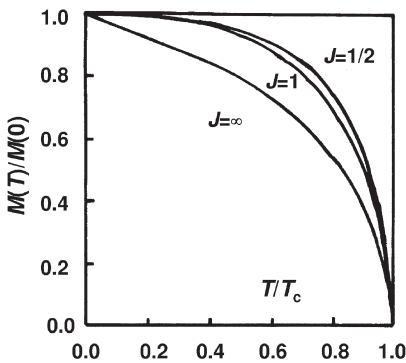


Figure 1.14 Spontaneous magnetization for $J = 1/2$, $J = 1$, and $J = \infty$.

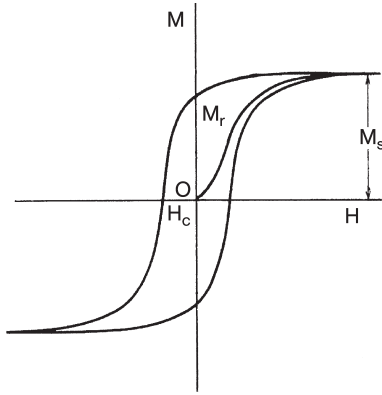


Figure 1.15 Hysteresis curve. Magnetization initially starts at the origin (O) and reaches its saturation magnetization (M_s). During the process of reducing magnetic fields, magnetization remains at $H = 0$ (M_r) and, for an opposite magnetic field, H_c , magnetization vanishes.

nal increasing curve, but remains at a certain value at $H = 0$. This is called the “residual magnetization” that corresponds to a genuine spontaneous magnetization. The reversed magnetic field gradually decreases the residual magnetization and finally makes the magnetization vanish at the field, $H = H_c$, which is named the “coercivity” or “coercive force”. The hysteresis loop is completed after a cyclic application of the magnetic field. The important parameters in the evaluation of the ferromagnetic materials consist of these three values, M_s , M_r , and H_c , and every combination of these parameters is useful for practical applications depending on the various targets. In particular, large M_r means a strong magnet, and the coercivity, H_c , discriminates the materials as either soft or hard magnets. A soft magnet is likely to be magnetized easily and is also easily demagnetized.

The initial unmagnetized state in ferromagnetic materials may need some elucidation. The magnetic domain model explains that, although each domain has spontaneous magnetization, the domains are arranged in such a manner as to cancel out the net magnetization. Once the magnetic field is applied, the domains move to the direction of the magnetic field. The magnetic domains are small regions, but may be observed by several methods. Fine magnetic particles are attracted onto the surface and image up to the domain boundary where the direction of the magnetic moments changes. Another method utilizes the magneto-optic effect using polarized light.

In the case of the antiferromagnetic ordered state, the two sublattices possess their own magnetizations, which are oriented in the opposite direction and at half the magnitude compared to the ferromagnetic case. However, each magnetization obeys the ferromagnetic spontaneous magnetization curve (see above, Figure 1.14) at half magnitude. Consequently, the net magnetization is almost zero, giving the same order of magnetic susceptibility as the paramagnetic state. The most important difference observed in this ordered state is the anisotropic susceptibilities, χ_{\parallel}

and χ_{\perp} , the parallel axis being defined along the magnetization direction, which is called an “easy axis”. Therefore, the external magnetic field can be applied along the easy axis or perpendicular to it and the magnetic susceptibilities, χ_{\parallel} and χ_{\perp} , are illustrated schematically in Figure 1.16, in which χ_{\parallel} decreases linearly toward zero on lowering the temperature, whereas χ_{\perp} stays constant. A powdered sample usually exhibits their averaged value,

$$\chi = (\chi_{\parallel} + 2\chi_{\perp})/3 \quad (1.65)$$

as plotted by the dashed line.

The most important magnetic behaviors of the antiferromagnets are the magnetic phase change with increasing magnetic field, especially a field applied along the easy axis; that is, the direction of the magnetic moments. The magnetic energy in the parallel arrangement (see Figure 1.16a) exceeds the assumed energy in the perpendicular arrangement (see Figure 1.16b) at a certain magnitude of the magnetic field, and the parallel orientation abruptly changes into the perpendicular one, conserving the antiparallel orientation. This magnetic phase change induced by the magnetic field is called the “flopping” of the magnetic moments or spins. Thus, the state is called the “spin-flopped” state, and the magnetic field which induces the transition is named the “critical field”, H_{cr} , or “spin-flop field”, H_{sf} . This magnetic phase transition depends on the anisotropic energy of the magnetic moment orientation. Theoretical consideration concludes the relation of H_{cr} with χ_{\parallel} and χ_{\perp}

$$H_{cr} = \sqrt{2K/(\chi_{\perp} - \chi_{\parallel})} \quad (1.66)$$

where K indicates the anisotropy constant, which causes the magnetic moments to align toward the easy axis in the absence of the magnetic field. Similarly, the

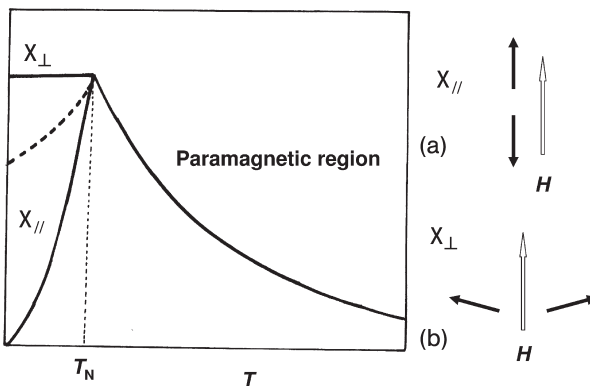


Figure 1.16 Magnetic susceptibility of an antiferromagnet. The dashed line indicates a powder susceptibility at the antiferromagnetic region, $T < T_N$.

antiferromagnetic arrangement of the magnetic moments is eventually unstable under high magnetic fields, and exhibits, to some extent, a tendency to approach the ferromagnetic state. Therefore, magnetization behavior in antiferromagnetic materials provide interesting magnetic properties with respect to the applied magnetic field. These phenomena are also important targets of magnetic investigations, and newly classified magnetism called metamagnetism is gathering much attention. The spin-flopped state can be referred to as antiferromagnetic resonance (AFMR), which will be dealt with later (see Section 3.6.3).

1.3.5

Magnetic Interactions

1.3.5.1 Exchange Interaction

Now we have prepared ourselves to have a deeper insight into various magnetic interactions between the magnetic moments. Let us consider two-electron systems, such as an He atom or a hydrogen molecule. As a result of spin multiplicity there exist singlet and triplet states and, therefore, four wave functions, ${}^1\Psi_0$, ${}^3\Psi_1$, ${}^3\Psi_0$, and ${}^3\Psi_{-1}$

$$\begin{aligned} {}^1\Psi_0 &= \frac{1}{\sqrt{2}}(|\phi_a\alpha\phi_b\beta\rangle - |\phi_a\beta\phi_b\alpha\rangle) \\ {}^3\Psi_1 &= |\phi_a\alpha\phi_b\alpha\rangle \\ {}^3\Psi_0 &= \frac{1}{\sqrt{2}}(|\phi_a\alpha\phi_b\beta\rangle + |\phi_a\beta\phi_b\alpha\rangle) \\ {}^3\Psi_{-1} &= |\phi_a\beta\phi_b\beta\rangle \end{aligned} \quad (1.67)$$

where ϕ_a and ϕ_b are orbital functions and α and β the spin function indicating $m_s = 1/2$ and $-1/2$, respectively. The total wave functions, including the orbital and spin functions, are represented by ‘‘Slater’s determinants’’. We focus our attention on the energy difference of the singlet and triplet states, evaluating the repulsion energy between the two electrons given by $\mathcal{H}' = (1/4\pi\epsilon_0)(e^2/r)$, where r is the distance between the two electrons. The kinetic and other potential energies of the two electrons with the nucleus constitute the Hamiltonian, \mathcal{H}_0 . The expectation values of \mathcal{H}_0 are the same for the two electrons, and we examine the expectation values of \mathcal{H} for the above-mentioned wave functions. Then we obtain the energies for ${}^1\Psi_0$ (E_S) and for ${}^3\Psi_1$, ${}^3\Psi_0$ and ${}^3\Psi_{-1}$ (E_T) as follows.

$$\begin{aligned} E_S &= C + J, & E_T &= C - J \\ C &= \frac{1}{4\pi\epsilon_0} \int \phi_a(1)\phi_b(2) \frac{e^2}{r} \phi_a(1)\phi_b(2) d\tau \\ J &= \frac{1}{4\pi\epsilon_0} \int \phi_a(1)\phi_b(2) \frac{e^2}{r} \phi_b(1)\phi_a(2) d\tau \end{aligned} \quad (1.68)$$

The integrals, C and J , are called the ‘‘Coulomb’’ and ‘‘exchange’’ integrals, respectively. The energy separation between the triplet and singlet states is $2J$, as

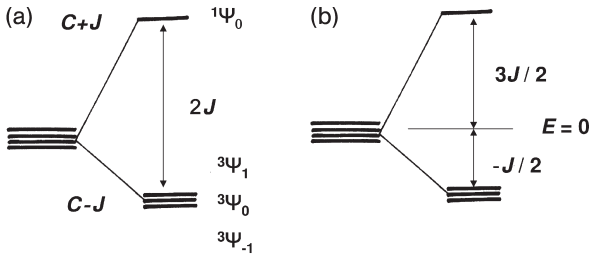


Figure 1.17 Energy shift due to Coloumb and exchange integrals and attributed to spin Hamiltonian, $-2JS_1 \cdot S_2$.

shown in Figure 1.17a. This quantum mechanical result is important because, when J is positive, the triplet states are more stable than the singlet state, meaning the ferromagnetic parallel spin is favorable. Considering that this energy-splitting originates from a difference in the spin multiplicity, we may put up the effective spin Hamiltonian as a phenomenological equivalence:

$$\mathcal{H}_{\text{ex}} = -2JS_1 \cdot S_2 \quad (1.69)$$

The eigenvalues of this Hamiltonian may be obtained by the operation of $S_1 \cdot S_2$ as $(3/2)J$ for the singlet state and $(-1/2)J$ for the triplet state, the separation being $2J$ (Figure 1.17b). Hex is called the “Heisenberg Hamiltonian” or a magnetic interaction of the Heisenberg type, expressing the exchange interaction between the electron spins. It is noted that the spin interaction of Heisenberg type is isotropic, as indicated by $S_1 \cdot S_2$.

In ferromagnetic or antiferromagnetic materials the following general expression is usual as an exchange interaction:

$$\mathcal{H}_{\text{ex}} = -2 \sum_{\langle ij \rangle} J_{ij} S_i \cdot S_j \quad (1.70)$$

As one can see from the r -dependence of the exchange integral, J , the magnitude of J_{ij} decreases quite rapidly depending on the distance r_{ij} between the electrons, i and j , and the nearest neighboring pairs are to be taken into account. Now the meaning of the Weiss molecular field, $H_{\text{mol}} = \Gamma M$, is comprehensible to be $H_{\text{mol}} = -2zJ\langle Sz \rangle / g_e \mu_B$, in which z is the number of the nearest neighboring spins and $\langle Sz \rangle$ the average value of Sz .

1.3.5.2 Dipolar Interaction

One more important magnetic interactions is called a “magnetic dipolar interaction”, given by the two magnetic dipoles or moments, m_1 and m_2 , as

$$U(m_1, m_2, r) = \frac{m_1 \cdot m_2}{r^3} - \frac{3(m_1 \cdot r)(m_2 \cdot r)}{r^5} \quad (1.71)$$

Here \mathbf{r} is a connecting vector between the two magnetic moments. This formula is a classical analog, but we replace \mathbf{m}_1 and \mathbf{m}_2 with explicit forms of the spin operators, \mathbf{S}_1 and \mathbf{S}_2 , leading to

$$\mathcal{H}(\mathbf{S}_1, \mathbf{S}_2, \mathbf{r}) = g_e^2 \mu_B^2 \left\{ \frac{\mathbf{S}_1 \cdot \mathbf{S}_2}{r^3} - \frac{3(\mathbf{S}_1 \cdot \mathbf{r})(\mathbf{S}_2 \cdot \mathbf{r})}{r^5} \right\} \quad (1.72)$$

Seeking the spin Hamiltonian of the magnetic dipolar interaction, the terms relevant to the orbital wave functions are integrated for an average, and then the above Hamiltonian is expressed in a tensor form as

$$\mathcal{H}_{SS} = g_e^2 \mu_B^2 [\mathbf{S}_{1x} \mathbf{S}_{1y} \mathbf{S}_{1z}] \cdot \begin{bmatrix} \left\langle \frac{r^2 - 3x^2}{r^5} \right\rangle & \left\langle \frac{-3xy}{r^5} \right\rangle & \left\langle \frac{-3xz}{r^5} \right\rangle \\ \left\langle \frac{-3xy}{r^5} \right\rangle & \left\langle \frac{r^2 - 3y^2}{r^5} \right\rangle & \left\langle \frac{-3yz}{r^5} \right\rangle \\ \left\langle \frac{-3xz}{r^5} \right\rangle & \left\langle \frac{-3yz}{r^5} \right\rangle & \left\langle \frac{r^2 - 3z^2}{r^5} \right\rangle \end{bmatrix} \cdot \begin{bmatrix} \mathbf{S}_{2x} \\ \mathbf{S}_{2y} \\ \mathbf{S}_{2z} \end{bmatrix} \quad (1.73)$$

Next we define the operator $\mathbf{S} = \mathbf{S}_1 + \mathbf{S}_2$, this expression is made up to

$$\mathcal{H}_{SS} = \frac{1}{2} g_e^2 \mu_B^2 [\mathbf{S}_x \mathbf{S}_y \mathbf{S}_z] \cdot \begin{bmatrix} \left\langle \frac{r^2 - 3x^2}{r^5} \right\rangle & \left\langle \frac{-3xy}{r^5} \right\rangle & \left\langle \frac{-3xz}{r^5} \right\rangle \\ \left\langle \frac{-3xy}{r^5} \right\rangle & \left\langle \frac{r^2 - 3y^2}{r^5} \right\rangle & \left\langle \frac{-3yz}{r^5} \right\rangle \\ \left\langle \frac{-3xz}{r^5} \right\rangle & \left\langle \frac{-3yz}{r^5} \right\rangle & \left\langle \frac{r^2 - 3z^2}{r^5} \right\rangle \end{bmatrix} \cdot \begin{bmatrix} \mathbf{S}_x \\ \mathbf{S}_y \\ \mathbf{S}_z \end{bmatrix} \quad (1.74)$$

This is finally expressed by the following spin Hamiltonian.

$$\mathcal{H}_{SS} = \mathbf{S} \cdot \mathbf{D} \cdot \mathbf{S} \quad (1.75)$$

Here \mathbf{D} is a 3×3 matrix and is called \mathbf{D} -tensor, satisfying $\text{Tr}[\mathbf{D}] = 0$. In the SI system, all relevant equations in the derivation must be multiplied by $\mu_0/4\pi$. This is a quantum mechanical expression of the magnetic dipolar interaction.

It is usually convenient to discuss the \mathbf{D} -tensor as a diagonalized form, and thus we have

$$\mathcal{H}_{SS} = Dx\mathbf{S}x^2 + Dy\mathbf{S}y^2 + Dz\mathbf{S}z^2, \quad Dx + Dy + Dz = 0 \quad (1.76)$$

Here Dx , Dy , and Dz are the principal values, and owing to $\text{Tr}[\mathbf{D}] = 0$, we define two independent parameters, D and E , as

$$D = \frac{3}{2}Dz, \quad E = \frac{1}{2}(Dx - Dy) \quad (1.77)$$

The transformation of (1.77) results in

$$\mathcal{H}_{SS} = D\left\{S_z^2 - \frac{1}{3}S(S+1)\right\} + E(S_x^2 - S_y^2) \quad (1.78)$$

The introduced parameters, D and E , are named the “zero-field splitting constants” after the fact that this interaction can split the spin states even in the absence of the external magnetic field. Eventually both parameters are given by the orbital integrations below:

$$\begin{aligned} D &= \frac{\mu_0}{4\pi} \frac{3}{4} g^2 \mu_B^2 \left\langle \frac{r^2 - 3z^2}{r^5} \right\rangle \\ E &= \frac{\mu_0}{4\pi} \frac{3}{4} g^2 \mu_B^2 \left\langle \frac{x^2 - y^2}{r^5} \right\rangle \end{aligned} \quad (1.79)$$

When we apply these relations to the delocalized system, the spin densities, ρ_i and ρ_j , are used:

$$\begin{aligned} D &= \frac{\mu_0}{4\pi} \frac{3}{4} g^2 \mu_B^2 \sum_{\langle ij \rangle} \frac{r_{ij}^2 - 3z_{ij}^2}{r_{ij}^5} \rho_i \rho_j \\ E &= \frac{\mu_0}{4\pi} \frac{3}{4} g^2 \mu_B^2 \sum_{\langle ij \rangle} \frac{x_{ij}^2 - y_{ij}^2}{r_{ij}^5} \rho_i \rho_j \end{aligned} \quad (1.80)$$

Then knowledge of the spin density and the distance vector \mathbf{r} between the two electrons makes it possible to evaluate the zero-field splitting constants, D and E .

Three important remarks are presented here: (1) this spin Hamiltonian is effective for $S \geq 1$; (2) this interaction produces a so-called “anisotropic energy”, which governs the preferential orientation of the spins or magnetic moments; (3) this is a point-dipole approximation. Comment (1) means this interaction vanishes in the case of $S = 1/2$. Concerning the second comment, the magnetic dipolar interaction works out uniaxially in symmetry for $E = 0$ and an orthorhombicity in symmetry becomes essential for $E \neq 0$. The final comment (3) is often utilized for an approximate evaluation of the distance, r , between the spins. Neglecting the spread of the electron wave functions, the representations of D and E are deduced as $E = 0$ and D , as follows:

$$D = \frac{3}{2} g^2 \mu_B^2 / r^3 \quad (1.81)$$

If the useful relation is expressed using $D/g\mu_B$ in mT and r in nm, then we have

$$D/g\mu_B = 1.391 g/r^3 \quad (1.82)$$

When $g = 2.0023$ and $r = 1$ nm, then this formula yields $D = 2.785$ mT.

1.3.6

Spin Hamiltonian

In the previous section we have discussed the magnetic interactions on the basis of electron spins and retained a deep insight into the magnetic interactions. The concept of a spin Hamiltonian was partially introduced and seems useful in pursuing investigations which are essentially associated with the electron spins, especially magnetism and electron spin resonance. Let us summarize here the fundamental Hamiltonians which determine the electronic states and their energies from the quantum mechanical point of view.

$$\mathcal{H} = \mathcal{H}_{\text{kin}} + \mathcal{H}_{\text{pot}} + \mathcal{H}_{\text{cr}} + \mathcal{H}_{\text{LS}} + \mathcal{H}_{\text{Ze}} + \mathcal{H}_{\text{spin}} \quad (1.83)$$

The first two terms concern the kinetic and the potential energies important for determining electronic orbital wave functions, and the third one is an energy derived from the crystal or ligand field that causes a shift of the electronic energy. The following two terms, \mathcal{H}_{LS} and \mathcal{H}_{Ze} , have been introduced as the spin-orbit coupling and the Zeeman energy, respectively. The final term includes every interaction regarding the electron spins. The exchange interaction, \mathcal{H}_{ex} , and the magnetic dipolar interaction, \mathcal{H}_{SS} , are its members, and in later chapters about magnetic resonance nuclear spin will be incorporated. In view of the orbital quenching we try to find an effective Hamiltonian by dealing with the two terms, \mathcal{H}_{LS} and \mathcal{H}_{Ze} , as a perturbation [3]

$$\mathcal{H}' = \lambda \mathbf{L} \cdot \mathbf{S} + \mu_{\text{B}} (\mathbf{L} + g_{\text{e}} \mathbf{S}) \cdot \mathbf{H} \quad (1.84)$$

The orbital wave functions are expressed as $|0\rangle, \dots, |n\rangle$, and their energies as E_0, \dots, E_n , are determined from $\mathcal{H}_0 = \mathcal{H}_{\text{kin}} + \mathcal{H}_{\text{pot}} + \mathcal{H}_{\text{cr}}$. The second-order perturbation results in

$$\mathcal{H} = \mu_{\text{B}} \mathbf{S} \cdot (g_{\text{e}} \mathbf{1} - 2\lambda \Lambda) \cdot \mathbf{H} - \lambda^2 \mathbf{S} \cdot \Lambda \cdot \mathbf{S} + \mu_{\text{B}}^2 \mathbf{H} \cdot \Lambda \cdot \mathbf{H} \quad (1.85)$$

Here Λ is a tensor which is composed of the matrix elements given by

$$\Lambda_{\mu\nu} = \sum_{n \neq 0} \frac{\langle 0 | \mathbf{L}_{\mu} | n \rangle \langle n | \mathbf{L}_{\nu} | 0 \rangle}{E_n - E_0}, \quad \mu, \nu = x, y, z \quad (1.86)$$

Concerning the Zeeman term, $\mathbf{1}$ is a unit matrix and the \mathbf{g} -tensor representation is convenient:

$$\mathbf{g} = g_{\text{e}} \mathbf{1} - 2\lambda \Lambda \quad (1.87)$$

Then the Zeeman Hamiltonian and the above result are written as follows:

$$\begin{aligned}\mathcal{H}_{Ze} &= \mu_B \mathbf{S} \cdot \mathbf{g} \cdot \mathbf{H} \\ \mathcal{H} &= \mu_B \mathbf{S} \cdot \mathbf{g} \cdot \mathbf{H} - \lambda^2 \mathbf{S} \cdot \mathbf{A} \cdot \mathbf{S} + \mu_B^2 \mathbf{H} \cdot \mathbf{A} \cdot \mathbf{H}\end{aligned}\quad (1.88)$$

Several points about these terms arise. Hereafter we call the \mathbf{g} -tensor a g -value, which is anisotropic, and is given by

$$g_{ij} = g_e \delta_{ij} - 2\Lambda_{ij} \quad (1.89)$$

Here δ_{ij} is a Kronecker δ . It is manifest that the anisotropy of g -value results from spin-orbit coupling, more precisely from the orbital contribution. The deviation of the g -value from the free electron and its anisotropy are undoubtedly evident in the ESR observations. It is interesting that the second term, $-\lambda^2 \mathbf{S} \cdot \mathbf{A} \cdot \mathbf{S}$, has a similar form to the magnetic dipolar interaction, $\mathcal{H}_{SS} = \mathbf{S} \cdot \mathbf{D} \cdot \mathbf{S}$. Considering the diagonalized Λ_{ij} , the formalism becomes the same so that this effect is included representatively in $\mathcal{H}_{SS} = \mathbf{S} \cdot \mathbf{D} \cdot \mathbf{S}$ (1.75). Therefore, the zero-field splitting parameters, D and E , are deduced, as given in (1.78). The second term, $-\lambda^2 \mathbf{S} \cdot \mathbf{A} \cdot \mathbf{S}$, is considered to be the result of a two-electron interaction of higher order as is seen from the fact that the validity of this relation is $S \geq 1$ and the term vanishes when $S = 1/2$. In addition, the nature of the anisotropy is also the same, and therefore a specific terminology is conferred as “one-ion anisotropy” or “one-ion anisotropy constant”. The last term (1.85) is independent of electron spins and indicates the higher order of orbital magnetic moments induced by the magnetic field. This is an origin of the van Vleck paramagnetism, which is independent of temperature. Summarizing all spin Hamiltonians we have

$$\mathcal{H} = \mu_B \mathbf{S} \cdot \mathbf{g} \cdot \mathbf{H} + \mathbf{S} \cdot \mathbf{D} \cdot \mathbf{S} - 2 \sum_{\langle ij \rangle} J_{ij} \mathbf{S}_i \cdot \mathbf{S}_j \quad (1.90)$$

1.3.7

Van Vleck Formula for Susceptibility

Here we deal with a general method for calculating magnetic susceptibility. When a substance is placed in an external field, its magnetization is given by its energy variation with respect to the field, $M = -\partial E / \partial H$. This magnetization is obtained by summing the microscopic magnetizations, m_n , weighted by the Boltzmann factors. Because an analogous relation for m_n also holds as

$$m_n = -\partial E_n / \partial H \quad (1.91)$$

it leads to the final formula

$$M = \frac{N \sum_n (-\partial E_n / \partial H) \exp(-E_n / kT)}{\sum_n \exp(-E_n / kT)} \quad (1.92)$$

where E_n ($n = 1, 2, 3, \dots$) is a quantum mechanical energy in the presence of the magnetic field, which will be fundamentally evaluated once the Hamiltonian of

the system is assumed. In this context the spin Hamiltonian discussed above for the magnetic interactions plays an important role. Thus, we require knowledge of E_n as a function of H . Van Vleck proposed some legitimate approximations, assuming the energy is an expansion in a series of the applied field [4, 5]:

$$E_n = E_n^{(0)} + E_n^{(1)}H + E_n^{(2)}H^2 + \dots \quad (1.93)$$

Where $E_n^{(0)}$ is the energy in zero field, the term linear to H is called the first-order Zeeman term, and $E_n^{(2)}$ the second-order Zeeman, that is

$$E_n^{(1)} = \langle n | \mathcal{H}_{Zc} | n \rangle, \quad E_n^{(2)} = \sum_{m \neq n} \langle n | \mathcal{H}_{Zc} | m \rangle^2 / (E_n^{(0)} - E_m^{(0)}) \quad (1.94)$$

where \mathcal{H}_{Zc} is as described in the previous section. The other nomenclatures are standard in perturbation theory. From (1.91) and (1.93) we have

$$m_n = -E_n^{(1)} - 2E_n^{(2)}H - \dots \quad (1.95)$$

The second approximation is the expansion of the exponential under $H/kT \ll 1$. This is fulfilled under the conditions of H not being too large and T not too low. The final form will be

$$M = \frac{N \sum_n (-E_n^{(1)} - 2E_n^{(2)}H)(1 - E_n^{(1)}H/kT) \exp(-E_n^{(0)}/kT)}{\sum_n (1 - E_n^{(1)}H/kT) \exp(-E_n^{(0)}/kT)} \quad (1.96)$$

The absence of the magnetization at zero magnetic field, $M = 0$, requires

$$\sum_n E_n^{(1)} \exp(-E_n^{(0)}/kT) = 0 \quad (1.97)$$

Substituting this relation into (1.96) and retaining only terms linear in H , finally we obtain the susceptibility given by

$$x = \frac{N \sum_n (E_n^{(1)2}/kT - 2E_n^{(2)}) \exp(-E_n^{(0)}/kT)}{\sum_n \exp(-E_n^{(0)}/kT)} \quad (1.98)$$

This is the “van Vleck formula”. When the states are degenerate, the summation is repeated n times, where n is a degeneracy. Let us explain how to utilize this formula and derive the analytical formulae of the magnetic susceptibility for several examples.

1.3.8

Some Examples of the van Vleck Formula

1.3.8.1 The Curie Law

Consider the spin degeneracy, S , with an orbital singlet, $L = 0$, the energy levels corresponding to the energy expansion in the derivation of the van Vleck formula are

$$E_n^{(0)} = 0, \quad E_n^{(1)} = g\mu_B m_S, \quad E_n^{(2)} = 0 \quad (1.99)$$

Then the result of χ (1.98) coincides with the Curie law of $\chi = Ng^2\mu_B^2 S(S+1)/3kT$.

1.3.8.2 Zero-Filed Splitting Case

In this case the following Hamiltonian is exemplified.

$$\mathcal{H} = \mu_B \mathbf{S} \cdot \mathbf{g} \cdot \mathbf{H} + \mathbf{S} \cdot \mathbf{D} \cdot \mathbf{S} \quad (1.100)$$

Here we assume the \mathbf{g} - and \mathbf{D} -tensors have the same principal axis and the rhombic parameter, E , is zero. The energies compared to the zero-field energy, $E_0 = 0$, will be given for the axial (parallel) direction of H as

$$E_1 = g_{\parallel} \mu_B H + D, \quad E_2 = -g_{\parallel} \mu_B H + D \quad (1.101)$$

Then the van Vleck formula for the parallel magnetic susceptibility is given by

$$\chi_{\parallel} = \frac{2Ng_{\parallel}^2 \mu_B^2}{kT} \frac{\exp(-D/kT)}{1 + 2\exp(-D/kT)} \quad (1.102)$$

When the magnetic field is perpendicular to the axial direction, the energies for the much larger D compared to the Zeeman energy become

$$E_1 = D, \quad E_2 = -g_{\perp}^2 \mu_B^2 H^2 / D, \quad E_3 = g_{\perp}^2 \mu_B^2 H^2 / D + D \quad (1.103)$$

As one can see from the relation, $E_n^{(1)} = 0$, for $n = 1, 2$, and 3 . The final result is

$$\chi_{\perp} = \frac{2Ng_{\perp}^2 \mu_B^2}{D} \frac{1 - \exp(-D/kT)}{1 + 2\exp(-D/kT)} \quad (1.104)$$

The temperature dependences of (1.102) and (1.104) and their inverse susceptibilities are drawn for certain parameters (Figure 1.18).

1.3.8.3 Spin Cluster Case—The Dimer Model

This model is expressed in the following Hamiltonian.

$$\mathcal{H} = -2J\mathbf{S}_1 \cdot \mathbf{S}_2 + g\mu_B(\mathbf{S}_{1z} + \mathbf{S}_{2z})H \quad (1.105)$$

The first term indicates the exchange-coupled two spins, $S_1 = S_2 = 1/2$, and the second term the Zeeman Hamiltonian in the applied magnetic field (this direction is specified by the z -axis). Consequently the spin system forms the singlet ($S = 0$) and triplet ($S = 1$) sublevels, the latter includes the energy terms dependent on the magnetic field. When the sign of J is negative, the energy diagram for the ground singlet and excited triplet energy is realized, as is often observed in actual cases

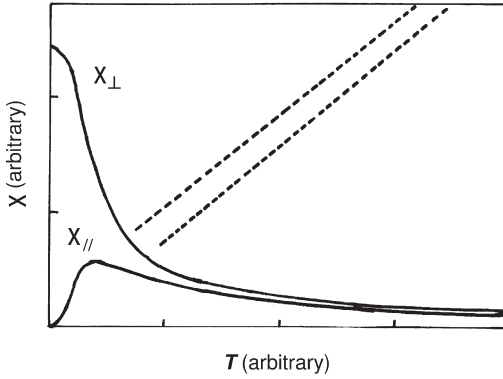


Figure 1.18 $\chi_{//}$ (1.102) and χ_{\perp} (1.104) in the case of $D > 0$. The dotted lines show that each inverse $1/\chi_{//}$ and $1/\chi_{\perp}$ follows a Curie–Weiss law above a certain temperature.

such as molecular magnetic materials or metal ion pairs. Thus, this model is well known as the “dimer” model or the “singlet–triplet” (ST) model. The energy of the four states is given as

$$\begin{aligned} E_1 &= (3/2)J \\ E_2 &= -(1/2)J + g\mu_B H, \quad E_3 = -(1/2)J, \quad E_4 = -(1/2)J - g\mu_B H \end{aligned} \tag{1.106}$$

The state, E_1 , is the singlet and E_2 , E_3 , and E_4 belong to the triplet. Applying the van Vleck formula, we obtain the magnetic susceptibility for the dimer model or ST model.

$$\chi = \frac{2Ng^2\mu_B^2}{3kT} \frac{\exp(-2|J|/kT)}{1 + 3\exp(-2|J|/kT)} \tag{1.107}$$

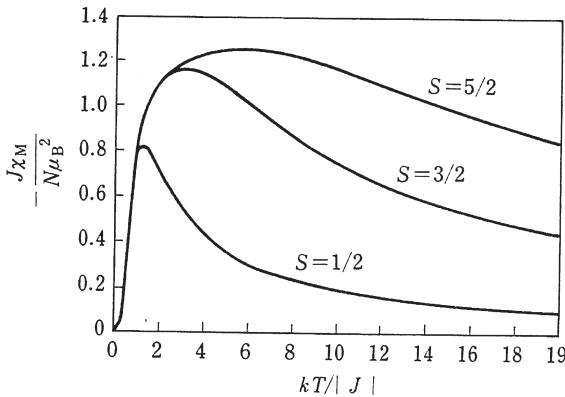


Figure 1.19 Dimer models in the case of $J < 0$ for $S = 1/2$ (ST model), $S = 3/2$, and $S = 5/2$.

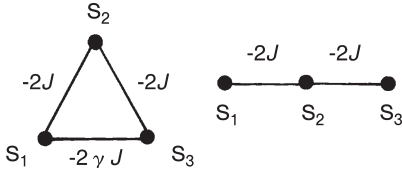


Figure 1.20 Triangle three-spin cluster and linear three-spin cluster.

Several temperature variations for $S = 1/2$, $S = 3/2$, and $S = 5/2$ pairs are shown in Figure 1.19, which are actually observed for the paired samples consisting of Cu^{2+} , Cr^{3+} , and Mn^{2+} ions.

1.3.8.4 Multiple-spin Cluster Case – The Triangle or Others

A group of interacting magnetic moments form a magnetic cluster and exhibit a prominent temperature-dependent magnetic susceptibility. For instance, triangle and linear trimer, square and linear tetramer, or star-burst spin networks are typical magnetic clusters. Even for these complicated spin systems the van Vleck formula works out efficiently, as long as appropriate Hamiltonians for the systems are deduced or presumed. Here we examine two cases consisting of three spins. The spin–exchange coupling structure is shown in Figure 1.20.

The spin–exchange interaction in an isosceles triangular three-spin system is expressed by the spin Hamiltonian:

$$\mathcal{H} = -2J(\mathbf{S}_1 \cdot \mathbf{S}_2 + \mathbf{S}_2 \cdot \mathbf{S}_3 + \gamma \mathbf{S}_3 \cdot \mathbf{S}_1) \quad (1.108)$$

In the case of $\gamma = 1$, it reduces to a regular triangle, whereas the linear trimer case corresponds to $\gamma = 0$. With the help of the Kambe formula [6] the magnetic susceptibility for $\gamma = 1$ leads to

$$\chi = \frac{Ng^2\mu_B^2}{4kT} \frac{5 + \exp(-3J/kT)}{1 + \exp(-3J/kT)} \quad (1.109)$$

In the regular triangle ($\gamma = 1$) with $J < 0$, it provides a strange situation, that is, one spin remains as a spin-frustrated state and this position is not designated in the ground state, thus presenting a spin frustration problem, which is an interesting target of research not only in theory but also in experiment. Space limitations mean we cannot discuss spin-clusters further here and the reader is referred to more magnetism-oriented books [4, 5].

1.3.8.5 Temperature-Independent Paramagnetism

Here we consider the ground state with $E_0^{(0)} = 0$ as an energy origin. In addition, it has no angular momentum and is therefore diamagnetic. Using $E_0^{(1)} = 0$ and $\chi = -2NE_0^{(2)}$ from the van Vleck formula, magnetic susceptibility is concluded to be given by

$$\chi = -2N \sum_{m \neq 0} \langle 0 | \mathcal{H}_{Ze} | m \rangle^2 / (E_0^{(0)} - E_m^{(0)}) \quad (1.110)$$

This relation indicates that the diamagnetic ground state may be coupled with the excited states by the second-order perturbation of the Zeeman Hamiltonian, eventually yielding paramagnetic susceptibility. All denominators in the equation are negative and no Boltzmann statistics are included so that the derived susceptibility features temperature-independent paramagnetism. This temperature-independent susceptibility, χ_{TIP} , is almost of the same order of magnitude of diamagnetism, although the sign is opposite, and it is actually observed in many materials. Materials containing the transition metal ions, in particular, exhibit a relatively large contribution, for instance $1\text{--}2 \times 10^{-4} \text{ emu mol}^{-1}$ for Ni^{2+} or Co^{3+} , having a singlet ground state, $^1A_{1g}$. The large contribution of χ_{TIP} is accounted for by the low-lying excited states coming from the factor, $1/(E_0^{(0)} - E_m^{(0)})$. It may be necessary to remark that temperature-independent paramagnetism is potentially generated from coupling between the ground state and the excited states, regardless of the ground state being diamagnetic or paramagnetic. In this context, for every paramagnetic material, χ_{TIP} is superimposed on the usual paramagnetism.

1.3.9

Low-Dimensional Interaction Network

When we consider magnetic interactions in the crystal, the magnetic networks of the interacting magnetic moments are generally three-dimensional. The exchange interaction shows dominant dependences on the distance between the two magnetic origins as well as on the electron distribution of the wave function in which the electron spins reside. Thus, the exchange interaction parameter, J , possesses the most remarkable value in a certain crystal direction. With this fact in mind, the magnetic interaction network in general is likely to become low-dimensional. These magnetic properties are categorized as low-dimensional problems, which attract much interest not only experimentally but also theoretically. In this sense one-dimensional magnetism, called “magnetic linear chains”, is most important. But sometimes we encounter layered magnetic systems as a two-dimensional model.

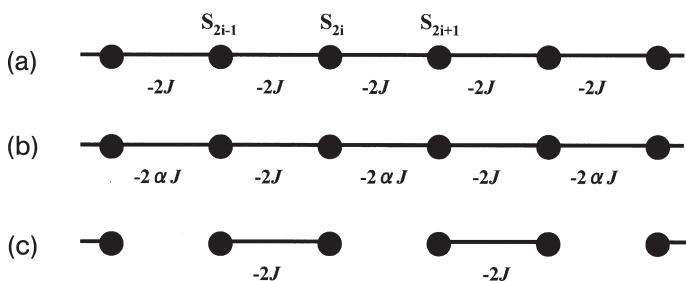


Figure 1.21 Magnetic interaction networks: (a) a regular linear chain; (b) an alternating linear chain; (c) dimer.

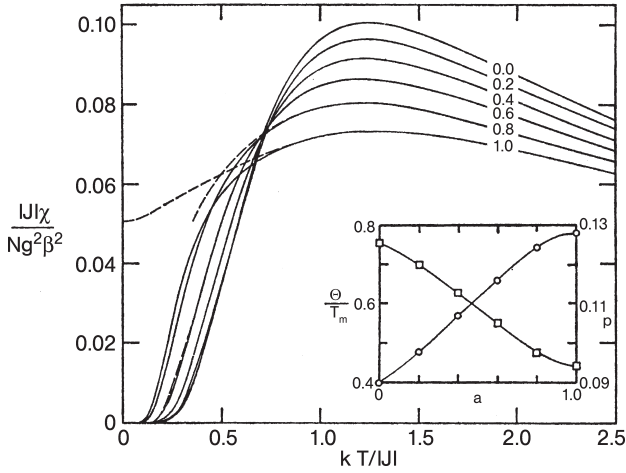


Figure 1.22 Magnetic susceptibilities for $\alpha = 1, 0.2, 0.4, 0.6, 0.8,$ and 1.0 in the one-dimensional magnetic chain. The calculations were made for a 10-spin chain in the Hamiltonian (1.111). The Bonner and Fisher case is $N \rightarrow \infty$ (the dashed line for $\alpha = 1.0$). The dimer ($S-T$) model is given by

$\alpha = 0$. The alternating chains correspond to $\alpha = 0.2-0.8$. The insert shows the Weiss constant divided by the temperature of the susceptibility maximum (circles) and the product of maximum susceptibility times the corresponding temperature, $p = \chi_{\max} k T_{\max} / N g^2 \mu_B^2$ (squares), versus α .

The expression “linear chain” refers to a magnetic chain within which each magnetic origin interacts with its two nearest neighbors only. The Hamiltonian of such a system will be given by using the exchange interaction of Heisenberg type, $-2J\mathbf{S}_1 \cdot \mathbf{S}_2$

$$\mathcal{H} = -2J \sum_{i=1}^{N/2} (\mathbf{S}_{2i-1} \cdot \mathbf{S}_{2i} + \alpha \mathbf{S}_{2i} \cdot \mathbf{S}_{2i+1}) \quad (1.111)$$

Depending on the sign of J , ferromagnetic and antiferromagnetic chains are possible as far as $\alpha > 0$. As is easily recognized, a variety of magnetic linear chains are available (Figure 1.21). The simplest case is $\alpha = 0$, the system being reduced to the dimer model, which of course is not characteristic of the magnetic chain. For $\alpha = 1$ the system conforms to an $S = 1/2$ uniform chain or “regular chain”. The magnetic susceptibility for antiferromagnetic chains was first calculated by Bonner and Fisher [7]. Data for $\alpha = 1$ (Figure 1.22) indicate unique behavior due to no energy gap above the ground state. The magnetic susceptibility reaches a maximum value, χ_{\max} , at the temperature, T_{\max} , given by

$$\chi_{\max} / (N g^2 \mu_B^2 / |J|) = 0.07346, \quad k T_{\max} / |J| = 1.282 \quad (1.112)$$

Below T_{\max} the susceptibility decreases gradually but it seems to remain constant towards the temperature of zero kelvin. According to Bonner and Fisher’s calculation the asymptotic susceptibility is expressed by the following relation:

$$\chi_{T=0}/(Ng^2\mu_B^2/|J|) = 0.05066 \quad (1.113)$$

The uniform ferromagnetic chain with $S = 1/2$ is expressed by [8]

$$\chi = (Ng^2\mu_B^2/4kT)\{1 + (J/kT)^a\} \quad (1.114)$$

with an exponent, a , depending on the temperature. For a high temperature limit like $kT/J > 1$, $a = 1$ and for $T \rightarrow 0$ a approaches $4/5$. A numerical expression is also proposed using $K = J/2kT$ as

$$\begin{aligned} \chi = (Ng^2\mu_B^2/4kT) \{ & (1 + 5.79599K + 16.902653K^2 + 29.376885K^3 \\ & + 29.832959K^4 + 14.036918K^5)/(1 + 2.79799K + 7.0086780K^2 \\ & + 8.6538644K^3 + 4.5743114K^4) \}^{2/3} \end{aligned} \quad (1.115)$$

On the other hand, the intermediate cases of $0 < \alpha < 1$ for $J < 0$ are classified as an alternating chain with strong and weak antiferromagnetic interactions, when it is known that the system has an energy gap. The calculations for these chains [9] are also depicted in Figure 1.22 above, together with the result of a regular linear chain. Due to the energy gap the magnetic susceptibilities tend to zero on lowering the temperature. Thus, we specify the linear chain models as the “regular” Heisenberg linear chain for $\alpha = 1$ and as the “alternating” Heisenberg chain for $0 < \alpha < 1$.

Some peculiar cases are described. One is the case of $\alpha < 0$, in which the alternating chain has both antiferromagnetic and ferromagnetic interactions. The magnetic susceptibility is numerically evaluated under some conditions. The other case is for $\alpha \rightarrow -\infty$, and then we have a regular chain with $S = 1$. This system is theoretically predicted to have a unique ground state with a gapped excitation spectrum. This gap is called the Haldane gap, and the magnetization curve at zero kelvin draws much attention from theoreticians and experimentalists as well.

Furthermore, the present magnetic chains interact with each other, forming a two-dimensional network with antiferromagnetic or ferromagnetic weak interactions. Among them, of course for special cases, a so-called uniform two-dimensional network is possible. These interchain interactions or two-dimensionality problems provide very interesting research subjects regarding the magnetic behavior of materials in comparison to the three-dimensional magnetic materials.

The following Hamiltonian is also noted:

$$\mathcal{H} = -2J \sum_{i=1}^N \{ \alpha \mathbf{S}_{zi} \mathbf{S}_{zi+1} + \gamma (\mathbf{S}_{xi} \mathbf{S}_{xi+1} + \mathbf{S}_{yi} \mathbf{S}_{yi+1}) \} \quad (1.116)$$

This Hamiltonian includes an anisotropic exchange effect except in the case of $\alpha = 1$ and $\gamma = 1$ of the Heisenberg exchange model. The most usual cases are of $\alpha = 1$ and $\gamma = 0$ or $\alpha = 0$ and $\gamma = 1$. These models are referred to as the “Ising” model and the “X–Y” model, respectively. The magnetic properties, including

thermal behaviours, may be analytically solved for the Ising model [10], and thus qualitative understandings on magnetism become possible. However, the Ising or X–Y model is applicable only for large anisotropic materials, such as Ni^{2+} and Co^{2+} , and, therefore, it is rare to analyse magnetic data from the standpoint of the Ising or X–Y model.

1.4 Experimental Magnetic Data Acquisition

1.4.1 Methods

Several methods (magnetometers) are utilized for the measurement of magnetic susceptibility. Historically, methods such as Gouy and Faraday methods, are classified as a “force method”. The force exerted on a sample for the Faraday method is given in the coordinates of Figure 1.1, shown earlier:

$$F_x = M_z \partial H_z / \partial x = v \chi H_z \partial H_z / \partial x \quad (1.117)$$

The determination of $H_z \partial H_z / \partial x$ is carried out by using known standard samples. The force direction coincides with gravity, so that a modified Faraday method, using a “torsion balance”, was invented, in which the field gradient is generated along the horizontal direction (see the y -axis in Figure 1.1). The horizontal torsion is canceled using an inductive coil set on the balance, where the feedback current is a measure of the force. The limit of the measurement amounts to $10^{-10} \text{ emu g}^{-1}$. Dynamic methods are also applicable; one is a vibrating sample magnetometer (VSM) and another is a magnetic induction method which involves applying an oscillating magnetic field. The detection systems consist of a detection coil by which the generated electromotive force, $V(t)$, or the mutual induction coefficient of the secondary coil (a Hartshorn bridge circuit is utilized) are measured, respectively. The latter method is important for determining the complex susceptibility, $\chi(\omega)$, which is given by

$$\chi(\omega) = \chi'(\omega) - i\chi''(\omega) \quad (1.118)$$

AC susceptibilities, in general, emphasize the magnetic loss or relaxation phenomena, and far more important is that $\chi''(\omega)$ is related to magnetic resonance phenomena, as an absorption of energy. The third method is based on the superconducting quantum interference effect. This magnetometer is called a SQUID (superconducting quantum interference device), which utilizes a superconducting ring with a weak-point junction, counting a quantized magnetic flux as a generated current (the Josephson effect). The SQUID magnetometer is commercially available and is the most prevalent method, and besides, data acquisitions in cgs units is very easy.

1.4.2

Evaluations of Magnetic Susceptibility and Magnetic Moment

The observed magnetic susceptibility comprises three main contributions

$$\chi_{\text{obs}} = \chi_{\text{para}} + \chi_{\text{TIP}} + \chi_{\text{dia}} \quad (1.119)$$

The first two terms are paramagnetic and the last one is diamagnetic, and the last two terms exhibit no temperature dependence. In order to evaluate the temperature-dependent χ_{para} and compare it with theoretical calculations, we have to subtract the other two contributions from χ_{obs} . The first thing to do is correction of diamagnetism. The term χ_{dia} may be evaluated by using appropriate substances which have a similar composition and molecular structure. However, this is not necessarily universal. Pascal allotted semiempirically diamagnetic susceptibilities of the composition atoms or atomic groups from the total diamagnetic observation (recent recommended values were summarized earlier in Table 1.2 [4, 5]). This validity is based on the additive law for each diamagnetic contribution. The next procedure is how to remove χ_{TIP} . For organic free radicals it may be negligible

Table 1.2a Diamagnetic susceptibilities of atoms and ions ($10^{-6} \text{ emu mol}^{-1}$).

H	-2.93	F	-6.3	Li ⁺	-1.0	F ⁻	-9.1
C	-6.00	Cl	-20.1	Na ⁺	-6.8	Cl ⁻	-23.4
N	-5.57	Br	-30.6	K ⁺	-14.9	Br ⁻	-34.6
N (in ring)	-4.61	I	-44.6	Rb ⁺	-22.5	I ⁻	-50.9
N (amide)	-1.54	S	-15.0	Cs ⁺	-35.0	CN ⁻	-13.0
N (diamide)	-2.11	Se	-23	NH ⁴⁺	-13.3	CNS ⁻	-31.0
O (alcohol, ether)	-4.61	P	-10	Mg ²⁺	-5.0	ClO ₄ ⁻	-32.0
O (carbonyl)	-1.73	As	-21	Ca ²⁺	-10.4	OH ⁻	-12.0
O (carboxyl)	-7.93	Si	-13	Zn ²⁺	-15.0	O ²⁻	-7.0
		B	-7	Hg ²⁺	-40.0	SO ₄ ²⁻	-40.1

Table 1.2b Diamagnetic susceptibilities of ligands and constitutive correction.

H ₂ O	-13	C=C	+5.5	CHCl ₂	+6.43
NH ₃	-18	C≡C	+0.8	CBr	+4.1
CO	-10	C=C-C=C	+10.6	Benzene	-1.4
CH ₃ COO ⁻	-30	C=C-C	+4.5	Cyclohexane	+3.0
Oxalate	-25	N=N	+1.85	Piperidine	+3.0
Pyridine	-49	C≡N	+0.8	Imidazole	+8.0
Bipyridine	-105	C=N	+8.15	C (tertiary)	-1.29
Pyrazine	-50	C=N-N=C	+10.2	C (quaternary)	-1.54
Ethylenediamine	-46	N=O	+1.7	C (one aromatic ring)	-0.24
Acetylanetonato	-52	CCl	+3.1	C (two aromatic rings)	-3.10
<i>o</i> -Phenanthroline	-128	CCl ₂	+1.44	C (three aromatic rings)	-4.0

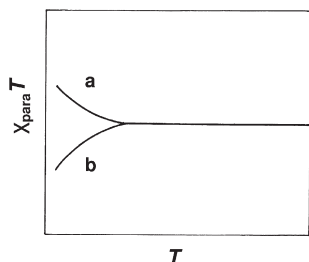


Figure 1.23 $\chi_{\text{para}} T$ - T plot. At low temperatures it deviates from (a) a constant line upward for ferromagnetic interaction and (b) downward for antiferromagnetic interaction. The constant value at higher temperature regions gives the effective magnetic moment, m_{eff} , and, accordingly, the spin quantum number of the sample.

because the orbital excited states lie far above the ground state. When we can assume or approximate the temperature dependence in the higher temperature region, a tactful method is applicable for deducing temperature-independent terms. Considering thermal agitation, the only constant contribution remains at $T \rightarrow \infty$. This asymptotic value corresponds to the remaining constant terms ($\chi_{\text{TIP}} + \chi_{\text{dia}}$).

The plot of the effective magnetic moment, m_{eff} , versus T from the obtained temperature-dependent χ_{para} is useful in knowing whether the magnetic interaction is ferromagnetic or antiferromagnetic and also what the magnetic moment or J (or S) value is. Considering the Curie law (1.54), m_{eff} can be evaluated from the asymptotic constant value at higher temperatures in the $\chi_{\text{para}} T$ - T plot (Figure 1.23). In lower temperature regions this plot deviates upward or downward, suggesting the ferromagnetic or antiferromagnetic interactions of the magnetic moments, respectively.

References

- 1 Spaldin, N.A. (2003) *Magnetic and Materials, Fundamentals and Device Applications*. Cambridge University Press, pp. 7, 16–17.
- 2 Henry, W.E. (1952) *Physical Review*, **88**, 559–62.
- 3 Pryce, M.H.L. (1950) *Proceedings of the Physical Society*, **A63**, 25–29.
- 4 Carlin, R.L. (1986) *Magnetochemistry*, Springer-Verlag, pp. 3, 20–21.
- 5 Kahn, O. (1993) *Molecular Magnetism*. VCH, Weinheim, pp. 3–7.
- 6 Kambe, K. (1950) *Progress of Theoretical Physics*, **5**, 48–51.
- 7 Bonner, J.C. and Fisher, M.E. (1964) *Physical Review*, **135**, A640–58.
- 8 Baker, G.A., Jr, Rushbrooke, G.S. and Gilbert, H.E. (1964) *Physical Review*, **135**, A1272–7.
- 9 Duffy, W. Jr and Barr, K. (1968) *Physical Review*, **165**, 647–54.
- 10 Onsager, L. (1944) *Physical Review*, **65**, 117–49.

